C. P. No. 556

C. P. No. 556

MINISTRY OF AVIATION

AERONAUTICAL RESEARCH COUNCIL

CURRENT PAPERS

Some Calculations by the Crocco-Lees and Other Methods of Interactions between Shock Waves and Laminar Boundary Layers, including Effects of Heat Transfer and Suction

By

K.N.C. Bray, G.E. Gadd and M. Woodger
Now of the Engineering Dept., Southampton University and of Aerodynamics Division and Mathematics Division, N.P.L. respectively

LONDON: HER MAJESTY'S STATIONERY OFFICE

1961

NINE SHILLINGS NET

C.P. No.556

Some Calculations by the Crocco-Lees and Other Methods of Interactions between Shock Waves and Laminar Boundary Layers, including Effects of Heat Transfer and Suction

- By -
K. N. C. Bray, G. E. Gadd and M. Woodger
Now of the Engineering Dept., Southampton University
and of Aerodynamics Division and Mathematics Division, N.P.L.
respectively

April, 1960

SUMMARY

The Crocco-Lees method is applied to interactions between shocks and boundary layers that remain laminar throughout. The underlying assumptions of the method are critically reviewed, and the mathematical analysis involved is presented. Results obtained by solving the resulting equations with the aid of the N.P.L. DEUCE computer are discussed. They are found to agree qualitatively with those of a more recent method. Cooling the wall and the use of distributed suction are both found to reduce the extent of regions of separation.

---

1. The Type of Problem to be Considered

Interactions between shock waves and boundary layers frequently occur in practice, but often the flow configuration is complicated. A basic understanding of such practical instances can, however, be gained by studying relatively simple cases. The cases to be considered in the present paper are those shown in Figs.1 and 2. It is assumed that the flow is two-dimensional, and that the boundary layer remains laminar throughout the region of interaction. This latter is an important assumption, since it is known that if transition occurs within the region of interaction it greatly affects the flow. However entirely laminar interactions are far from academic, since high-speed aircraft usually fly high, with correspondingly low Reynolds numbers.

Heat transfer between the airstream and the surface often arises in practice, and it can have a large effect on the interaction. Hence cases with heat transfer are studied in the present paper. Distributed suction is also considered as it may be of practical interest in the future.

2. Introductory Outline of the Crocco-Lees Method

The theoretical method used in the major part of the paper is that due to Crocco and Lees[1,2,3,4]. An account will be given in this section of the underlying approximations and physical assumptions of the method.

Consider the cases shown in Fig.1 or Fig.2. Here the pressure rise imposed on the boundary layer by the incident shock, or by the change of wall slope, has an influence on the flow upstream of the shock or corner. The pressure begins to rise above its upstream value, and this causes the boundary layer to thicken, because near to the wall there is a region of

low-speed/

Previously issued as A.R.C.21,834.

low-speed subsonic flow. The thickening of the boundary layer deflects the external flow outwards from its original direction, so generating a band of compression waves. Clearly the boundary-layer thickening must be matched to the associated compression waves, and finding the conditions under which the two processes can be in equilibrium constitutes the principal task of any theory of shock wave boundary-layer interaction.

According to the theory, the pressure distributions at the wall upstream and downstream of the point of shock impingement in Fig.1 will be identical with those upstream and downstream of the corner in Fig.2 if the pressures and external-flow Mach numbers at large distances upstream and downstream are the same. Experiment[5] shows that in fact, the upstream influence is considerably bigger for the case of Fig.1. Hence the assumptions which imply the identity of the two cases are suspect. These assumptions concern the nature of the flow near the point where the shock strikes the boundary layer in Fig.1 or near the corner in Fig.2. Thus it is assumed for Fig.2 that the profile of the velocity component parallel to the wall is the same just downstream of the corner as just upstream of it, though in reality it seems quite likely that the corner would cause abrupt proportional changes in the speed of the slowest-moving fluid, thus changing the shape of the profile near the wall. Likewise in Fig.1 it is assumed that the shock reflects locally as an expansion, which is such as just to cancel the rise of pressure through the incident shock. Whilst this is broadly true, the detailed manner in which the shock penetrates into the layer and reflects from it is not reproduced in the analysis, which assumes the process to be compressed into a point. Also the velocity profile is assumed to suffer no abrupt changes on passing under the point of shock impingement, and this assumption, like the corresponding one in the case of Fig.2, may be in error.

It is easiest to discuss the method in connection with Fig.2, though the arguments only require slight modification to be applied to Fig.1. In inviscid flow a shock wave would spring from the corner in Fig.2, but the boundary layer has a "softening" effect, so that near the wall there is a band of compression waves, which only coalesce into a shock further out. Hence outside the boundary layer, but near the wall, the pressures and flow directions are related to each other by the simple-wave flow relations. It is assumed that the boundary layer has a definite edge, along which the simple-wave flow relations apply, and that between this edge of the layer and the wall, the pressure is constant along lines perpendicular to the wall. These assumptions are not strictly compatible close to the corner, but they are nearly so if the change of wall direction at the corner is fairly small. This would normally be the case for interactions involving entirely laminar layers, since a large change of flow direction would probably cause transition to occur before the boundary layer reattached. However, the assumption concerning the pressure within the boundary layer is open to more serious objections. In reality the boundary layer has no definite edge, so this is defined somewhat arbitrarily. If it is chosen so as to include too great a proportion of supersonic flow, the boundary layer so defined would grow thinner on encountering a rise in pressure, because such a rise would cause the supersonic stream tubes to contract. A thinning of the layer is incompatible with the generation of compression waves in the external flow. In the terminology of Crocco and Lees the boundary layer would be "supercritical", whereas if defined as normally, so as to include a smaller proportion of supersonic flow, the laminar boundary layer is "subcritical". The root of the trouble is the assumption that within the boundary layer the pressure gradient is zero normal to the wall. In reality the boundary layer merges gradually with the inviscid outer flow, and in the outer, supersonic, part of the layer, the pressure and the flow angle tend to be constant along Mach lines rather than along lines perpendicular to the wall. It is because of this that the outer-flow streamlines can converge whilst at the same time turning away from the wall. A similar situation arises with regard to turbulent layers, where there is little latitude in the definition of the edge, and the layer is

nearly/

nearly always "supercritical" according to the theory. This leads to an apparent fundamental distinction between laminar (subcritical) and turbulent (supercritical) layers, whereas in reality there is no such absolute physical difference. For both types of layer, a rise of pressure causes the inner, slow-moving, stream tubes to expand, and this deflects the outer flow away from the wall.

Although the arbitrariness in the definition of the edge of the laminar layer may seem from the above discussion to involve great uncertainties in any results of the theory, it will be seen later that "reasonable" choices for the edge give results that are in fair agreement.

It is necessary to relate the thickening of the boundary layer, and the consequent deflection of the external flow, to the pressure distribution. This is done by integrating the equations of continuity and momentum across the layer. The resulting equations are combined, and put into a form involving certain parameters. These parameters depend on the shape of the velocity and temperature profiles, and accordingly they vary through the region of interaction. Relations between the parameters are obtained as follows. Suppose the considerations of the equilibrium between the outer flow and the boundary layer, governing the pressure distribution, as discussed above, could be set aside. Then if the wall temperature were the same at all points, and a special form of pressure distribution could be imposed on the layer, the profiles would not vary in shape with distance along the wall, but only the thickness of the layer would vary. For incompressible flow the distribution of external velocity needed to produce these "similar" profiles is of the form $U = kx^n$, and a more complicated family of pressure distributions, related to the incompressible lower-law family by the Stewartson transformation[6], produces the same result in compressible flow. For these special distributions, the parameters of the Crocco-Lees method would take on values that would not vary with distance along the wall, but would depend only on the index n of the equivalent power-law velocity distribution, and on the ratio of the absolute temperature at the wall to the stagnation temperature. This ratio would be unity for zero heat transfer, since the Prandtl number is assumed to be unity. If there is distributed suction through the wall, varying with position along the wall in such a way as to maintain similar profiles, the parameters would, in addition, be dependent on a factor related to the rate of suction. Thus, the parameters in these circumstances could be regarded as functions of one of their number, of the wall-temperature ratio, and of the suction factor. These same relationships are assumed to apply for general types of pressure distribution, and this assumption makes the integration of the equations possible. It is thus, for example, assumed that the shape of the velocity profile at separation is fixed, and is the same as that at reattachment.

Thus the essence of the Crocco-Lees method is seen to be this, that by suitable manipulation the equations are reduced to a form involving as unknowns certain parameters whose interrelationships can plausibly be assumed to be relatively simple. This procedure differs in no essential respect from the well-known method of Pohlhausen for low-speed flow, based on the von Kármán momentum integral equation. The parameters arising in that equation are different from those of the Crocco-Lees method, but they are related in the same way to a one-parameter family of profiles, such as the similar-profiles family. It may seem at first sight to be a fundamental difference between the two methods that one of the parameters of the Crocco-Lees method should be concerned with the entrainment of air from the external flow into the boundary layer. This focusses attention on the way that the higher velocity external-flow air mixes with the slower-moving air in the boundary layer, so giving up to it some of its momentum, and for this reason the theory was originally described as a "mixing" theory. This fundamental physical process may appear to be completely overlooked in the Pohlhausen method. However, account is taken of it because a similar transfer of momentum takes place at points within the boundary layer, as well as at its edge, and the von Kármán momentum integral equation is the mathematical expression of just this overall process. Thus no absolute fundamental difference is involved.

There/

There is, however, the following distinction. A usual feature of methods of the Pohlhausen type is that not only the integral of the equation of momentum across the boundary layer is satisfied, but also the equation itself is satisfied at the wall. In this way the curvature of the velocity profile at the wall is related to the local pressure gradient. The other shape parameters of the profile are assumed to be related to the profile curvature at the wall. In the Crocco-Lees method the equation of motion is not satisfied at the wall, but in place of this there is introduced the condition that the rate of entrainment of fluid into the boundary layer from the external stream is related to the shape of the velocity and temperature profiles. No parameter depending on the curvature of the velocity profile at the wall is used. This is a point in favour of the method, since the overall characteristics of the profile shape are far from uniquely related to its curvature at the wall. On the other hand, the dependence of the Crocco-Lees method on an arbitrary definition of the edge of the layer is an unsatisfactory feature that is absent in methods of the Pohlhausen type. Moreover, whilst it is not obvious which characteristic of profile shape determines the rate of entrainment of the external fluid, it seems quite likely to be associated with the curvature of the outer parts of the velocity profile, so that it may be no more closely related than the curvature at the wall to the broad, overall shape of the profile, as expressed by parameters such as K.

The relationships between the Crocco-Lees parameters as used in the N.P.L. calculations differ in an important respect from those proposed originally, and used in earlier calculations[7,8]. The differences occur in the values of the parameters for separated layers. Originally, the profiles for such layers were treated as though there were an inner region of motionless flow, whilst the outer part of the velocity profile was assumed to be the same in shape as the profile at the separation point. However, amongst the similar-profile solutions, there are certain profiles, called "lower-branch" solutions, which resemble the profiles of separated layers, as they have a region of reversed flow near the wall. Stewartson[9] first drew attention to the possible use of these solutions as a representation of the flow in a separated region. They have been used in the present calculations both because they seem better founded than the original forms, and because they give rise to predicted pressure distributions whose general shape agrees better with experiment. A further, but minor, difference between the N.P.L. calculations and the earlier ones is that in our work viscosity is assumed to be proportional to absolute temperature. This assumption is in any case involved in the Stewartson transformation, which is used in deriving the theory, and its adoption somewhat simplifies the analysis.

To summarize, then, the main assumptions and approximations of the Crocco-Lees method are as follows:

(1) Boundary-layer theory is applicable, the pressure being treated as constant across the layer.

(2) Details at the point of shock impingement (Fig.1) or near the corner of the wall (Fig.2) are only of local importance.

(3) The velocity and temperature profiles may be taken to belong to a family of "similar solutions", from which the basic parameters are derived.

(4) The equations which are to be satisfied are based on continuity considerations, on a momentum integral relation, and on an equation relating the thickening of the boundary layer to the pressure distribution.

3. The Equations Used

Four basic parameters are used in the Crocco-Lees method, chosen in such a manner that according to the Stewartson transformation the

relationship/

relationship between them will be independent of Mach number. The first of these parameters is K, which depends on the shape of the velocity and temperature profiles, and is defined as

$$K = \frac{I}{mu_e}, \qquad \ldots (1)$$

where $I = \int_0^\delta \rho u^2 \, dy$, the momentum flux in the boundary layer, $m = \int_0^\delta \rho u \, dy$, the mass flux in the boundary layer, suffix e denotes conditions at the "edge" of the boundary layer, and δ (equal to y_e) is the "total" thickness of the layer. A second parameter, C, is related to the entrainment of fluid into the boundary layer from the mainstream, from which entrainment is subtracted any removal of fluid from the boundary layer by suction at the wall. C is defined by

$$C = \frac{m}{\mu_e} C_M = \frac{m}{\mu_e} \left\{ \frac{d\delta}{dx} - \phi - C_Q \right\}, \qquad \ldots (2)$$

where ϕ is the angle between the wall and the streamlines at the edge of the boundary layer, C_M may be termed the "mixing coefficient", and C_Q is the suction coefficient, $- \rho_w v_w / \rho_e u_e$, where suffix w denotes conditions at the wall. A parameter σ, related to the ordinary coefficient of local skin friction C_f, is defined as

$$\sigma = \frac{mC_f}{2(1 - K)C\mu_e} \qquad \ldots (3)$$

A final "shape" parameter, ψ, depends on the Mach number at the edge of the boundary layer and on the shapes of the velocity and temperature profiles, and is equal to

$$\psi = t\left(\frac{\rho_e u_e \delta}{m} - K \right), \qquad \ldots (4)$$

where t is the ratio of the temperature at the edge of the boundary layer to the free-stream stagnation temperature.

These four parameters, K, C, σ and ψ, arise in the equations in the following way.

It follows directly from the definition of C_M (equation (2)) that

$$\frac{dm}{dx} = \rho_e u_e C_M. \qquad \ldots (5)$$

By integrating with respect to y from 0 to δ the momentum equation of the boundary layer, viz.

$$\rho u \frac{\partial u}{\partial x} + \rho v \frac{\partial u}{\partial y} = \rho_e u_e \frac{du_e}{dx} + \frac{\partial}{\partial y}\left(\mu \frac{\partial u}{\partial y} \right),$$

and making use of the equation of continuity,

$$\frac{\partial (\rho u)}{\partial x} /$$

$$\frac{\partial(\rho u)}{\partial x} + \frac{\partial(\rho v)}{\partial y} = 0,$$

we obtain

$$\frac{dI}{dx} = u_e \frac{dm}{dx} + \delta \rho_e u_e \frac{du_e}{dx} - \tau_w + \rho_e u_e^2 C_Q, \qquad \ldots (6)$$

where τ_w is the shear stress at the wall. It is assumed in deriving equation (6) that δ is sufficiently great for the shear stress at δ to be virtually zero and the velocity at δ to be virtually equal to u_e. This sets a lower limit on δ. An upper limit is set by the requirement, discussed in the previous section, that too great a region of supersonic flow should not be included within the region, from $y = 0$ to $y = \delta$, over which the pressure is assumed to be a function only of x.

From equations (1) to (6)

$$\frac{dK}{dx} = \frac{B}{m}\frac{dm}{dx} + \frac{\psi}{w_t}\frac{dw}{dx}, \qquad \ldots (7)$$

where $B = (1 - K)(1 - \sigma) + C_Q/C_M$, $w = u_e/a^\circ$ (a reduced free-stream velocity), and a° is the stagnation speed of sound.

Another basic equation can be regarded as arising from the interaction between the boundary layer and the isentropic outer flow. It states that the rate of boundary-layer growth, $d\delta/dx$, as calculated from the free-stream deflection angle, must be equal to the value of $d\delta/dx$ calculated from the chosen boundary-layer parameters. As already discussed, the boundary layer is considered to have a well-defined edge δ, which is the dividing line between it and the isentropic outer flow. From the definition of the mixing-rate coefficient C_M in equation (2)

$$\frac{d\delta}{dx} = C_M + \phi + C_Q. \qquad \ldots (8)$$

The angle ϕ is related to the supersonic outer-flow velocity by the simple-wave-flow equations. For these we use a second-order approximation, namely

$$\phi = \left(1 - \frac{w}{\bar{w}}\right)\left(a + b\frac{w}{\bar{w}}\right), \qquad \ldots (9)$$

where $a \equiv (\bar{M}^2 - 1)^{\frac{1}{2}} - b$,

$$b \equiv \frac{\gamma-1}{4}(\bar{M}^2 - 1)^{\frac{3}{2}} + \frac{\gamma-1}{2}(\bar{M}^2 - 1)^{\frac{1}{2}} + \frac{\gamma+1}{4}(\bar{M}^2 - 1)^{-\frac{1}{2}},$$

$\bar{w} \equiv$ value of w when $\phi = 0$,

$\bar{M} \equiv$ Mach number corresponding to $\bar{w}$.

Replacing ϕ in equation (8) from equation (9), we have our first expression for $d\delta/dx$, in terms of the outer-flow velocity.

Before considering the second expression for $d\delta/dx$ it should be noted that in equation (9), when the analysis is applied to the situations of Figs.1 or 2, there are two possible values of $\bar{w}$. One of these, w_o, is the

value/

value of w corresponding to flow parallel to the wall upstream of the shock or corner, and the other value, w_∞, corresponds to flow parallel to the wall downstream of the shock or corner. Thus in Fig.1 the direction of the w_∞ flow is the same as that of the w_o flow, but w_∞ is less than w_o because of the incident and reflected shocks. In Fig.2, on the other hand, w_∞ is less than w_o because the direction of the w_∞ flow is inclined upwards to that of the w_o flow. Upstream of the shock or corner w_o will be used for $\bar{w}$ in equation (9), and downstream, w_∞ will be used.

The second expression for $d\delta/dx$ comes from the definition of the parameter ψ in equation (4), which may be written

$$m = \frac{t\rho_e u_e \delta}{\psi + Kt} . \qquad \ldots (10)$$

Since the external flow is isentropic, $t = 1 - (\gamma - 1)w^2/2$ and $td\rho_e/dx = -\rho_e w\, dw/dx$. If ψ is regarded as a function of K, we obtain, by differentiating (10) with respect to x and eliminating dK/dx, from (7),

$$\frac{d\delta}{dx} = \frac{\delta}{\psi+Kt}\left\{\frac{1}{m}\frac{dm}{dx}\left[B\frac{d\psi}{dK} + \psi - t\sigma(1-K) + t + t\frac{C_Q}{C_M}\right] + \frac{1}{wt}\frac{dw}{dx}\left[\psi\frac{d\psi}{dK} + J\right]\right\}, \qquad \ldots (11)$$

where $J \equiv \gamma w^2\psi + Kt\,(w^2 - t)$. Setting this equal to equation (8) gives the required interaction equation. However, before writing this down we proceed to define a dimensionless mass-flow variable

$$\zeta \equiv \frac{m}{\mu^o} , \qquad \ldots (12)$$

where superscript o denotes free-stream stagnation conditions, and a dimensionless x-wise distance

$$X \equiv \frac{(x - x_s)}{\delta_s} , \qquad \ldots (13)$$

where δ_s is the boundary-layer thickness at the separation point, and x_s the value of x there. In terms of these new variables the interaction equation becomes

$$\frac{1}{wt}\frac{dw}{dX}\left[\psi\frac{d\psi}{dK} + J\right] + \frac{1}{\zeta}\frac{d\zeta}{dX}\left[B\frac{d\psi}{dK} - E\right] = 0, \qquad \ldots (14)$$

where $E \equiv \dfrac{t\phi}{C_M} + t\sigma\,(1 - K) - \psi.$

Finally, if we assume that $\mu \propto T$ so that $\mu_e/\mu^o = t$, the equations of continuity (5) and momentum (7) may be written

$$\frac{d\zeta}{dX} = \frac{\gamma\delta_s p^o}{\mu^o a^o}\,\frac{p}{p^o}\,\frac{Cw}{\zeta} \qquad \ldots (15)$$

and/

and
$$\frac{dK}{dX} = \frac{B}{\zeta}\frac{d\zeta}{dX} + \frac{\psi}{wt}\frac{dw}{dX} \qquad \ldots (16)$$

4. The Relations between the Parameters

As discussed in Section 2, the parameters of the Crocco-Lees method, K, C, σ and ψ, are treated as functions of one of their number, and of the factors determining the wall temperature and the amount of suction. The relationships between the parameters are obtained from the similar solutions of the boundary-layer equations. These similar solutions can be derived in a form which does not explicitly contain Mach number by means of the Stewartson transformation[6], which can be written

$$\left.\begin{aligned} \bar{y} &= \frac{a_e}{a_d\sqrt{\nu_d}}\int_o^y \frac{\rho}{\rho_d}\,dy, \qquad \bar{x} = \int_o^x \left(\frac{a_e}{a_d}\right)^{\frac{3\gamma-1}{\gamma-1}} dx, \\ \frac{\partial s}{\partial y} &= \frac{\rho u}{\rho_d\sqrt{\nu_d}}, \qquad \frac{\partial s}{\partial x} = -\frac{\rho v}{\rho_d\sqrt{\nu_d}} \end{aligned}\right\} \qquad \ldots (17)$$

Here s is a stream function, so that the continuity equation is satisfied, and suffix d stands for some datum position. For a Prandtl number of 1, the equations of motion and energy can be written

$$\rho u\frac{\partial u}{\partial x} + \rho v\frac{\partial u}{\partial y} = \rho_e u_e\frac{du_e}{dx} + \frac{\partial}{\partial y}\left(\mu\frac{\partial u}{\partial y}\right)$$

and
$$\rho u\frac{\partial H}{\partial x} + \rho v\frac{\partial H}{\partial y} = \frac{\partial}{\partial y}\left(\mu\frac{\partial H}{\partial y}\right),$$

where H is the ratio of the total temperature, $T + u^2/2C_p$, to the total temperature in the free stream. If viscosity is proportional to absolute temperature, so that $\rho\mu$ is constant across the boundary layer, the Stewartson transformation applied to these equations yields

$$\frac{\partial^2 s}{\partial\bar{y}\partial\bar{x}}\frac{\partial s}{\partial\bar{y}} - \frac{\partial^2 s}{\partial\bar{y}^2}\frac{\partial s}{\partial\bar{x}} = H\left(\frac{\partial^2 s}{\partial\bar{y}\partial\bar{x}}\frac{\partial s}{\partial\bar{y}}\right)_e + \frac{\partial^3 s}{\partial\bar{y}^3} \qquad \ldots (18)$$

and
$$\frac{\partial s}{\partial\bar{y}}\frac{\partial H}{\partial\bar{x}} - \frac{\partial s}{\partial\bar{x}}\frac{\partial H}{\partial\bar{y}} = \frac{\partial^2 H}{\partial\bar{y}^2}. \qquad \ldots (19)$$

Assume now that we can write

$$\left.\begin{aligned} s - s_w &= \frac{2^{\frac{1}{2}}K^{\frac{1}{2}}}{(n+1)^{\frac{1}{2}}}\bar{x}^{\frac{n+1}{2}}F(\eta), \qquad s_w = \frac{2^{\frac{1}{2}}K^{\frac{1}{2}}}{(n+1)^{\frac{1}{2}}}\bar{x}^{\frac{n+1}{2}}G, \qquad H = H(\eta), \\ \text{where} \quad \eta &= K^{\frac{1}{2}}\left(\frac{n+1}{2}\right)^{\frac{1}{2}}\bar{x}^{\frac{n-1}{2}}\bar{y}, \end{aligned}\right\} \qquad \ldots (20)$$

suffix w stands for conditions at the wall ($\eta = 0$), and

$$F', H \to 1 \text{ as } \eta \to \infty; \quad F = F' = 0, \quad H = H_w \text{ at } \eta = 0 \qquad \ldots (21)$$

These/

These substitutions of course imply a special form of external-velocity distribution, a special type of distribution of the suction velocity through the wall, and a wall temperature that is constant. Under these restrictive conditions the equations (18) and (19) reduce to

$$F''' + FF'' + \beta(H - F'^2) + GF'' = 0 \qquad \ldots (22)$$

and

$$H'' + (F + G)H' = 0, \qquad \ldots (23)$$

where $\beta \equiv 2n/(n + 1)$. This shows that the assumption underlying relations (20), that the profiles of s and H as functions of $\bar{y}$ can be similar in shape for all values of $\bar{x}$, is in fact compatible with equations (18) and (19). For the special conditions under which these similar solutions are valid, the parameters of the Crocco-Lees method can be shown from the definitions given in equations (1) to (4) and from equation (5) to be given by

$$\left.\begin{aligned} K &= F_e^{-1}\int_0^{\eta_e} F'^2\,d\eta \doteqdot 1 - C^{-\frac{1}{2}}\int_0^{\infty} F'(1 - F')d\eta \\ C &= F_e^2 \doteqdot \left[\eta_e + \int_0^{\infty}(H - 1)d\eta - \int_0^{\infty}(H - F')d\eta\right]^2 \\ \sigma &= F''(o)/(1 - K)C^{\frac{1}{2}} \\ \psi &= F_e^{-1}\int_0^{\eta_e} H\,d\eta - K \doteqdot C^{-\frac{1}{2}}\int_0^{\infty}(H-F')d\eta + C^{-\frac{1}{2}}\int_0^{\infty} F'(1-F')d\eta \end{aligned}\right\} \qquad (24)$$

Also C_Q/C_M, involved in the term B of equations (14) and (16), is given by

$$\frac{C_Q}{C_M} = \frac{G}{F_e} \qquad \ldots (25)$$

The edge values, distinguished by suffix e, in equations (24) and (25) are the values at η_e, where $F'(\eta_e)$ takes an arbitrary constant value close to 1. The usual value taken for $F'(\eta_e)$ is 0.95, as this is found[7] to give the best agreement with Lighthill's asymptotic solution[10] for the behaviour at the upstream end of the region of interaction. Some calculations have been done in the present paper, however, with $F'(\eta_e) = 0.98$. There is no theoretical reason why $F'(\eta_e)$ should be taken as constant throughout the interaction region, though varying it would greatly increase the complexity of the calculations. However, it will be seen later that re-calculating a case using a constant value of 0.98 in place of the normal constant value of 0.95 makes little overall difference to the results. Hence it is reasonable to assume that a constant value of 0.95 is satisfactory for general use.

It follows from (21), (22) and (23), that for the similar solutions K, C, σ, ψ and C_Q/C_M are functions only of β, H_w and G. Thus K, C, σ and C_Q/C_M can be regarded as functions of ψ, H_w and G. These relationships are assumed still to apply even when the conditions regarding the external-velocity distribution, etc., necessary for similar solutions are no longer satisfied. In this more general context H_w, being the ratio of the absolute temperature of the wall to the absolute stagnation temperature of the free stream, still has a clear significance, but G becomes merely a parameter related to the rate of suction. If G is treated as a constant,

as it is for any particular case in the present calculations, the suction coefficient C_Q will vary from point to point in a way that can only be determined after the computations have been completed. This is discussed further in section 6 below.

Solutions of equations (22) and (23) under the boundary conditions (21) have been given by Hartree[11], Cohen and Reshotko[12], and Stewartson[9] and by other workers. Cohen and Reshotko give many results for cases without suction but with various values of H_w. It is for convenience in the use of Cohen and Reshotko's data that the approximate forms have been included in equations (24): Cohen and Reshotko tabulate the quantities $\int_0^\infty (H - 1)d\eta$, $\int_0^\infty (H - F')d\eta$, $\int_0^\infty F'(1 - F')d\eta$ and $F''(0)$; also $F'(\eta)$, from which it is easy to determine η_e.

Some of the results tabulated by Cohen and Reshotko correspond to so-called "lower-branch" solutions of equations (22) and (23). It is found that for negative values of β that are not too large in magnitude there are two solutions of equations (22) and (23) having the correct asymptotic behaviour for large values of η. One of these solutions has a lower value of skin friction than the other, and is called the lower-branch solution. Such solutions have been investigated in detail by Stewartson[9] for the case $H = 1$, $G = 0$, corresponding to zero heat transfer and suction. Usually the skin friction is actually negative with lower-branch solutions, so that there is a region of reversed flow near the surface, like there is with a well-separated boundary layer. Values of the Crocco-Lees parameters corresponding to lower-branch solutions can of course be calculated just as easily as for the upper-branch solutions, and it seems logical to use them between separation and reattachment. When the Crocco-Lees theory was first formulated, however, it was argued that between separation and reattachment K, C and σ would remain constant at their separation values. This is equivalent to the assumption that the velocity profile has a region of zero velocity close to the wall, joined on to an outer profile which is of the same shape as the complete profile at separation. Results obtained on this assumption differ markedly for well-separated flows from those obtained using lower-branch values of the parameters in the separated regions. The latter type of result is more in line with experiment, and hence the majority of the calculations have been carried out with parameter tables that include lower-branch values.

To compute the functions for cases without suction, the data given by Cohen and Reshotko had to be supplemented by data drawn from Stewartson's study[9] of lower-branch solutions for the case $H_w = 1$. With the edge of the boundary layer defined in the usual way as the point where $F' = 0.95$, K, C, σ and ψ were calculated and graphs drawn as in Figs.3 to 5, for the five values of H_w (0, 0.2, 0.6, 1.0 and 2.0) considered by Cohen and Reshotko. The curves for $H_w = 0.6$ were extrapolated in conformity with the adjacent curves, and values were read from the graphs and tabulated as in Tables 1 and 2 for the conditions $H_w = 1.0$ and $H_w = 0.6$ for which calculations have been done. The former condition corresponds to cases with no heat transfer or suction, whilst the latter corresponds to cases without suction but with the wall cooled to 0.6 times the absolute stagnation temperature of the free stream.

One case was calculated using functions which were in accordance with the original idea that K, C and σ must remain constant between separation and reattachment. The table used was almost the same as Table 1 between the constant-pressure and separation conditions, though there were

small/

small differences due to attempting to make the curves join smoothly onto the conditions of constant K, C and σ beyond separation.

Another case was calculated for $H_w = 1$, $G = 0$, as above, but with a different edge definition, $F' = 0.98$ instead of 0.95. The corresponding functions are given in Table 3.

Finally, cases with $H_w = 1$, i.e., no heat transfer, but with distributed suction such that $G = 0.4$ were considered. The data for this condition had to be calculated from new solutions of the basic equation (22), since existing solutions were not available.* The computations were carried out by Mr. A. R. Curtis of Mathematics Division, N.P.L., using the DEUCE computer to solve the differential equation by a method of successive approximation. Separation was found to occur when $\beta = -0.3719$, as compared with the value -0.1988 without suction or heat transfer. Table 4 shows the calculated Crocco-Lees parameters. Since the term C_Q/C_M enters the equations (14) and (16), and is equal to $G/F_e = G/C^2$, it was found more convenient to tabulate $F_e^{-1}(\psi)$ than $C(\psi)$, as this avoided an unnecessary square-root calculation at each step in the integration of the equations. Also it was necessary to tabulate $(1 - K)\sigma$ rather than σ. This was because values of K above and below 1 were obtained for the case with suction, whereas without suction K is always less than 1, at any rate over the range of the tables; when $K = 1$, $\sigma(\psi)$ has a singularity, as can be seen from equations (24). The values of K greater than 1 were obtained for lower-branch profiles with large reversed-flow regions. In such a region F' is negative, and if there is sufficient reversed flow, $\int_0^\infty F'(1 - F')d\eta$ can be negative, so that K exceeds 1 by equations (24), despite the positive contribution to the integral made by the outer part of the profile.

5. Details of the Computational Methods

5.1 Cases without suction

The equations to be solved, derived from equations (14) and (16), are dealt with in the following form:

$$\frac{d\psi}{d\zeta} = \frac{JB + \psi E}{\zeta(JK' + \psi)}, \qquad \frac{dw}{d\zeta} = \frac{wt(-B + K'E)}{\zeta(JK' + \psi)} \qquad \ldots (26)$$

where $t = 1 - 0.2\,w^2$

$J = 1.4\psi w^2 + Kt(w^2 - t)$

$B = (1 - K)(1 - \sigma)$

$E = C^{-1}\zeta\phi + (1 - K)\sigma t - \psi$

$\phi = (1 - w/\bar{w})(a + bw/\bar{w})$

$b = 0.1\,(\bar{M}^2 - 1)^{\frac{3}{2}} + 0.2\,(\bar{M}^2 - 1)^{\frac{1}{2}} + 0.6\,(\bar{M}^2 - 1)^{-\frac{1}{2}}$

$a = (\bar{M}^2 - 1)^{\frac{1}{2}} - b$

$\bar{M}/$

---

*It was subsequently discovered that a few solutions for $G = 0.4$ had previously been found by Dr. L. Fox and quoted in an unpublished paper, A.R.C.12,699, by Dr. B. Thwaites.

$$\bar{M} = \bar{w}(1 - 0.2\bar{w}^2)^{-\frac{1}{2}}$$

$$\bar{w} = \begin{cases} w_0 & \text{upstream of shock in Fig.1 or corner in Fig.2 } (\zeta < \zeta_1) \\ w_\infty & \text{downstream of shock or corner } (\zeta > \zeta_1) \end{cases}$$

$$K' = \frac{dK}{d\psi} \text{ is derived from the table of } K(\psi)$$

K, C, σ are tabulated functions of ψ

$$w_0 = M_0(1 + 0.2M_0^2)^{-\frac{1}{2}}$$

This pair of non-linear ordinary differential equations for ψ and w in terms of ζ involves a parameter (see below) which has to be determined so as to satisfy the boundary conditions at infinity upstream and downstream of the shock or corner. We have thus an "eigenvalue" problem, and the large amount of computing required to determine the parameter necessitates the use of automatic computing aids.

A particular case will be determined by specifying the free-stream Mach number M_0, the value ζ_s of ζ at separation, and either (a) the condition that the shock strength or change of wall slope is just sufficient to cause separation, so that separation and reattachment both occur at $\zeta = \zeta_s$, at the point where the shock strikes the boundary layer in Fig.1 or at the corner in Fig.2, or (b) a value of w_∞ which defines the pressure rise downstream of the shock or corner.

Considering first the region upstream of separation ($\zeta < \zeta_s$), the parameter to be determined is w_s, the value of w at that point. For various values of w_s the corresponding solutions for ψ and w are found by stepwise integration upstream from separation.

The prescribed boundary condition is that $d\psi/d\zeta$ shall tend to zero as ζ becomes sufficiently less than ζ_s, i.e., far upstream of the interaction. This alone would not appear to define a unique solution for w_s, but the solutions for ψ turn out to have the following characteristic properties which do enable w_s to be determined uniquely, at least for values in a physically meaningful range. ψ decreases monotonically upstream and downstream from the shock, for values of w_s sufficiently close to the true one. If w_s is too large ψ deviates to $+\infty$ exponentially after a certain stage; if w_s is too small ψ deviates to $-\infty$ exponentially after a certain stage. w behaves in the same way. The true solutions for w and ψ lie below the positively deviating solutions and above the negatively deviating ones, these being practically coincident for longer ranges of ζ below ζ_s the more nearly the corresponding initial values of w_s lie to the true value. Both ψ and w do in fact tend to virtually constant limiting values when w_s is sufficiently well determined, so that the boundary condition is satisfied as far as possible. However, equations (26) show that ψ and w cannot remain perfectly constant over the whole distance between the leading edge ($\zeta = 0$) and some point well upstream of the region of interaction (see Section 6). For this would require $B = E = 0$ over this range of ζ, and hence the product $\zeta\phi$, which occurs in E, would have to be constant. Hence ϕ would vary with ζ, which is incompatible with the constancy of w.

The/

The upstream behaviour of the solution ψ is exploited as follows in determining w_s efficiently. An initial guess is provided for w_s, together with an initial correction δ (not to be confused with boundary layer thickness) to be applied to w_s after the first integration run. (δ expresses the most probable uncertainty in the initial guess, and too large or too small a value of δ can greatly increase the subsequent amount of computation). After successive integration runs $+\delta$ or $-\delta$ is added to w_s as appropriate until the true w_s has been bracketed, which is revealed by one solution going to $+\infty$ and the next to $-\infty$, or vice versa. At this stage δ is halved on each successive run and its sign changed as appropriate, until w_s has been determined within a prescribed accuracy δ_o, chosen in the light of experience so as to ensure that ψ has reached its upstream limiting value. To detect the onset of exponential deviation by an automatic method use is made of a further observed property of the solutions ψ, namely that $d\psi/d\zeta$ is never negative upstream of the shock for the true solution, so that a negative value indicates positive deviation. Negative deviation is detected by ψ going below the range of the tabulated functions $K(\psi)$, $C(\psi)$, $\sigma(\psi)$, which is well below the upstream limiting (constant pressure) value. An earlier method of detecting deviation was based on the assumption that $d\psi/d\zeta$ decreased in absolute value throughout a run, but this was found to be false in many cases for the larger Mach number.

Having determined w_s and hence the functions $w(\zeta)$ and $\psi(\zeta)$ for $\zeta < \zeta_s$ by upstream integrations from the separation point there are two distinct problems to be solved by stepwise integration downstream of this point (i.e., for $\zeta > \zeta_s$). The first is to determine the parameter w_∞ so that the shock strength or change of wall slope is just sufficient to cause separation, i.e., so that separation, shock or corner, and reattachment all occur at ζ_s. This is quite analogous to the upstream problem, ψ decreasing monotonically to a constant value if w_∞ has been correctly chosen and deviating exponentially to $+\infty$ or $-\infty$ according as w_∞ was too large or too small. In the second type of downstream problem a value of w_∞ is prescribed, somewhat less than that obtained for the first problem, and one has to find a value of ζ_1, the position of the shock or corner, such that ψ tends to a constant value far downstream. In this case ψ increases from ζ_s up to the shock or corner, at which point the value of $\bar{w}$ is changed abruptly and ψ begins to decrease again. The parameter ζ_1 is adjusted so as to postpone the exponential deviation of ψ just as before, an increase of ζ_1 tending to produce upward deviation of ψ and a decrease of ζ_1 a downward one.

The quantities of practical interest are not the variables ζ, ψ and w convenient for the numerical treatment of the problem but quantities related to the derived functions $X = (x - x_s)/\delta_s$ (distance downstream from separation as a ratio to the thickness of the boundary layer at separation, $P = p/p^\circ$ (pressure ratio in terms of stagnation pressure) and $\Delta = \delta/\delta_s$ (boundary layer thickness normalized to unity at separation). To produce values of X the following third differential equation obtained from equations (10), (12) and (15) is integrated at the same time as the others.

$$\frac{d\bar{X}}{d\zeta} = \frac{\zeta}{CPw}, \qquad \bar{X} = 0 \text{ at } \zeta = \zeta_s \qquad \ldots (27)$$

where/

where

$$P = t^{\frac{7}{2}}$$

$$\Delta = c\zeta(\psi + Kt)/Pw$$

$$c = (\zeta_s(\psi_s + K_s t_s)/P_s w_s)^{-1}$$

$$X = c\,\bar{X}$$

The integration was carried out on the N.P.L. automatic computer DEUCE, using floating-point arithmetic and a second-order Runge-Kutta integration routine. The interval of integration in ζ was fixed for each case and determined in the light of experience to give the accuracy required. It was found adequate to use downstream of the separation point an interval of twice that used upstream, and to increase the interval for increased values of ζ_s. Downstream intervals of 4, 8, 8 were used for $\zeta_s = 250, 560, 1250$ respectively. Since the bulk of the work is in calculating the quantities appearing in the differential equations at each step and only rough data is available for the functions K, C, σ it was thought best to use a low-order Runge-Kutta formula for the sake of speed. The quantities ψ, w and $\bar{X}$ at ζ_1 are obtained from their values at the adjacent integration steps by linear interpolation, to start the integration downstream from the shock.

To save time the values of the quantities at successive steps are not punched out from DEUCE until the parameter (w_s or w_∞ or ζ_1 as the case may be) has been determined to the desired accuracy. At the end of each trial run a single card is punched bearing the value of the parameter used, the correction applied to it, and the values of ζ and ψ at run termination. Finally, two complete sets of quantities for each step are punched out, an "upper bound" solution with ψ ultimately increasing exponentially and a "lower bound" solution with ψ ultimately decreasing exponentially. For each step the quantities X, Δ, P, ζ, ψ, w are available, punched on a single card in binary scale. Conversion to decimal form is carried out on a separate run.

One programme was arranged to find w_s and automatically go on to determine w_∞ for just separated flow, and another to find ζ_1 corresponding to given w_∞, using w_s found by the first programme. A simple modification to the second programme enabled it to be used to perform a single integration run from separation to shock or corner (ζ_1 specified) which is very quick. This is all that is required in certain practical cases where the onset of turbulent flow near the shock or corner renders the downstream pressure distribution of academic interest only.

The computing time was between one and two seconds per step. With a good initial guess at w_s and w_∞ the total time for the first programme would be typically 20 minutes for 10 integration runs (of 60 steps each) finding w_s to sufficient accuracy, 4 minutes for 8 runs (of 15 steps each) finding w_∞, and conversion to decimal would take another 13 minutes. It was found necessary to determine w_s to better than four decimal places and w_∞ to four in order to obtain a reasonably long downstream run before deviation of ψ and w. For the second programme the value of w_∞ specified is critical - if it is too small ψ goes above the range of the table, or else reattachment may never take place (the overall pressure ratio being too great) and much machine time may be wasted waiting for the run to terminate; however, a typical run might take from 7 to 15 minutes for 7 runs finding ζ_1 plus 5 to 10 minutes for conversion.

In/

In view of the very approximate nature of the data available for the functions $K(\psi)$, $C(\psi)$, $\sigma(\psi)$ and the necessity for referring to them twice per step during the course of the calculations an attempt was made to compress the tables into a small storage space on the machine. Linear interpolation was used to reduce the computing time and the number of instructions to be stored. The range of ψ was divided into two parts somewhere near the minimum value of K, the functions being stored at equal intervals of ψ in the two ranges. The lower range of ψ corresponds mainly to attached flow in which the second derivatives of the functions with respect to ψ are larger than in the separated region, so a smaller interval of ψ was necessary there. By storing only the increase of each function above its minimum value in the range, to an accuracy of one part in a thousand, one tabular entry for all three functions was accommodated within 30 binary digits in a single "word" on DEUCE, and the 32 words of one track of the magnetic drum store sufficed to contain the whole table. $K'(\psi)$ was calculated from the table of $K(\psi)$ using four adjacent tabular entries. Each programme comprised 37 tracks of instructions and data.

5.2 Cases with distributed suction

The equations to be solved differ from those given under (5.1) only in the addition of the term G/F_e to B. To avoid an unnecessary square root calculation at each step the function $F_e^{-1}(\psi)$ was tabulated instead of $C(\psi)$, as already mentioned in Section 4, and the formulae which involved C or σ were expressed instead in terms of F_e^{-1} and $(1 - K)\sigma$.

The behaviour of w and ψ upstream of separation in these suction cases was more abrupt than hitherto, and it was necessary to divide the interval of integration by four. ψ'' had a distinct negative region. Downstream of separation it was sufficient to halve the interval.

A rather remarkable phenomenon appeared when a solution was attempted using too large an interval, which would be noticed at once in hand computation but gave a misleading impression using an automatic computer until its possibility was appreciated. The solution showed convergence of ψ to a constant value in an apparently smooth fashion, and slight changes of w_s from the apparently correct eigenvalue had the appropriate effect on ψ. But the limiting value of ψ was too high, as revealed by halving the interval, and w_s was also too large. The second order Runge-Kutta process derives the increment of ψ over each integration step from a weighted average of derivatives computed at the initial and two-thirds-step points. It turned out that in the spurious solution ψ approached the limiting value in such a way that the derivatives at the initial and two-thirds-step points were large and of opposite signs, so that they cancelled out to give a small increment for ψ over the whole step. In this case a table of differences of ψ suggested the necessity for reducing the interval, although a graph did not.

6. The Relations for Reynolds Number, Displacement and Momentum Thicknesses, Upstream and Downstream Pressures, and Suction Coefficient

In the previous section it was shown how the DEUCE computer produces values of $P = p/p^\circ$ and $\Delta = \delta/\delta_s$ as functions of $X = (x - x_s)/\delta_s$. It may be more useful to present the results in the form of graphs of P, R_{δ^*} and R_θ as functions of R_x, where the R's are the Reynolds numbers $\rho_o u_o \delta^*/\mu_o$, $\rho_o u_o \theta/\mu_o$ and $\rho_o u_o x/\mu_o$ respectively. Here suffix o denotes conditions in the free-stream flow parallel to the wall upstream of the shock or corner, $\delta^* = \int_o^\infty \left(1 - \frac{\rho u}{\rho_e u_e}\right) dy$, the

displacement/

displacement thickness, $\theta = \int_0^\infty \frac{\rho u}{\rho_e u_e}\left(1 - \frac{u}{u_e}\right) dy$, the momentum thickness, and x is the distance from the leading edge.

From the definitions of δ^* and θ it follows that $\delta^* = \delta - m/\rho_e u_e$ and $\theta = m(1 - K)/\rho_e u_e$. Hence from equations (10) and (12) and the fact that the external flow is isentropic

$$R_{\delta^*} = \frac{w_o t_o^{1.5}}{w t^{1.5}} \frac{\zeta[\psi - (1 - K)t]}{t^2} \qquad \ldots (28)$$

$$R_\theta = \frac{w_o t_o^{1.5}}{w t^{1.5}} \frac{\zeta(1 - K)}{t}, \qquad \ldots (29)$$

and

$$R_x = R_{xs} + \frac{w_o t_o^{1.5}}{w_s t_s^{1.5}} \frac{\zeta_s(\psi_s + K_s t_s)X}{t_s^2} \qquad \ldots (30)$$

where suffix s denotes the separation point.

As discussed in the preceding section, ψ and w both tend to approximately constant values upstream of the region of interaction. Since w is almost constant, ψ tends to a close approximation to ψ_c, the value for the constant-pressure boundary layer. However w is not quite the same as w_o, the value for flow parallel to the wall, because of the growth of the boundary layer. The term E in equations (26) is approximately zero upstream: hence $\phi \doteq \frac{C_c}{\zeta}[\psi_c - (1 - K_c)\sigma_c t_o]$. But since w is close to w_o,

$$\phi \doteq (M_o^2 - 1)^{\frac{1}{2}}\left(1 - \frac{w}{w_o}\right).$$

Hence

$$\frac{w}{w_o} = 1 - \frac{C_c[\psi_c - (1 - K_c)\sigma_c t_o]}{\zeta(M_o^2 - 1)^{\frac{1}{2}}}. \qquad \ldots (31)$$

This is only a slowly varying function of ζ if ζ is large. Corresponding to equation (31)

$$\frac{p}{p_o} = 1 + \frac{\gamma M_o^2 C_c[\psi_c - (1 - K_c)\sigma_c t_o]}{\zeta(M_o^2 - 1)^{\frac{1}{2}}} \qquad \ldots (32)$$

This expression can also be derived from equation (28), since

$$\frac{p}{p_o} = 1 + \frac{\gamma M_o^2}{(M_o^2 - 1)^{\frac{1}{2}}}\left[\frac{d\delta^*}{dx} - C_Q\right].$$

If ζ is large, p is only slightly greater than p_o unless M_o is very large, when the "hypersonic leading-edge effect" occurs. Equations (31) and (32) also apply far downstream of the region of interaction, if suffix o values are replaced by the corresponding suffix ∞ ones.

From/

From equation (15)

$$x = \frac{\mu^o a^o}{\gamma p^o} \int_0^\zeta \frac{\zeta d\zeta}{PCw} .$$

Hence upstream of the region of interaction, where $\psi \div \psi_c$ and w is not very different from w_o,

$$R_x = \frac{\rho_o u_o x}{\mu_o} \div \frac{\zeta^2}{2C_c t_o^2} = \frac{(1 + 0.2M_o^2)^2 \zeta^2}{2C_c} \qquad \ldots (33)$$

The formula only applies upstream. Denoting such a position by suffix u, we have, by combining with equation (30),

$$R_x = \frac{(1 + 0.2M_o^2)^2 \zeta_u^2}{2C_c} + \frac{w_o t_o^{1.5}}{w_s t_s^{1.5}} \frac{\zeta_s[\psi_s + K_s t_s](X - X_u)}{t_s^2} . \qquad \ldots (34)$$

Both terms on the right-hand side of this equation vary with X_u, which may be chosen arbitrarily in the upstream region where the pressure is virtually constant. However it is found that the sum of the two terms remains unaffected by the choice of X_u, as is of course to be expected.

For cases with suction it follows from equations (2), (12), (24) and (25) that the suction coefficient, C_Q, is given by

$$C_Q = GtC^{\frac{1}{2}}\zeta^{-1} . \qquad \ldots (35)$$

Hence upstream of the region of interaction $C_Q \div Gt_o C_c^{\frac{1}{2}} \zeta^{-1}$, and from equation (33),

$$C_Q = \frac{G}{\sqrt{2R_x}} . \qquad \ldots (36)$$

The cases with suction in the present paper have all been calculated with a constant value of G equal to 0.4. This is for convenience. If, by contrast, C_Q were kept constant, the labour of the computation would be greatly increased because it would be necessary to solve equation (35) concurrently with equations (26) to determine G, which would now be variable, and also the basic similar profiles would have to be computed over a range of values of G, and the appropriate Crocco-Lees parameters found by interpolation at every step in the calculations. With G kept constant the distribution of suction velocity is rather artificial, the suction velocity varying as $x^{-\frac{1}{2}}$ upstream of the region of interaction. However equation (35) shows that C_Q does not vary greatly over the region of interaction. The average rate of mass flow per unit area sucked into the wall between the leading edge and separation is, from equation (36), about $2^{\frac{1}{2}} G R_x^{-\frac{1}{2}}$ times the rate of mass flow per unit area in the free stream, whilst locally over the region of interaction the ratio of the mass-flow rates is about $2^{-\frac{1}{2}} G R_x^{-\frac{1}{2}}$. Thus we may say that the case calculated is roughly equivalent to a case with uniform suction with a suction coefficient $\overline{C_Q}$, where

$$2^{-\frac{1}{2}} G R_{xs}^{-\frac{1}{2}} < \overline{C_Q} < 2^{\frac{1}{2}} G R_{xs}^{-\frac{1}{2}} . \qquad \ldots (37)$$

7./

7. Results

The cases that have been computed by the Crocco-Lees method are set out in Table 5.

Case 1, with $M_o = 2$, is the same as a case computed by Bray[7], except that in parts of his analysis he does not assume the Prandtl number to be 1, or the viscosity to be proportional to absolute temperature, though other parts of his analysis imply these simplifying assumptions, which are made consistently throughout the present paper. The table of functions used by Bray and for Case 1 is that originally proposed by Crocco and Lees, and differs from Table 1 beyond separation, where it was originally assumed that K, C and σ remain constant, no account being taken of the lower-branch similar solutions. It can be seen from Figs.6 and 7 that the present results agree fairly well with Bray's, despite the slight differences in the equations used. The points S, C and R in these and subsequent figures denote the position of separation, of the corner in Fig.2 or the point where the shock strikes the boundary layer in Fig.1, and of reattachment. The Reynolds number R_{xs} at separation is usually specified beforehand in the examples worked out, and C is then that position of the corner or shock which provokes separation at S for the given overall pressure ratio, (i.e., for the given change of wall slope at C). Thus in Figs.6 and 7 $w_\infty = 1.3615$ and $w_o = 1.4907$, corresponding to an incident shock (Fig.1) with a flow-deflection angle of about 4° or a change in wall slope (Fig.2) of about 8°. For other cases with incipient separation, where the calculation is to find w_∞ just small enough to cause separation, the points C and R coincide with S.

It can be seen from the curves for Case 2 in Figs.6 and 7 that the use of the parameters given in Table 1, based on lower-branch values, rather than the original table of parameters, leads to a large difference in the shape of the pressure distributions when as in the present instance, there is an extensive region of separation. The lower-branch parameters give rise to a much more rapid falling off of pressure gradient downstream of separation. In Fig.6 the pressure gradients in fact become negative upstream of the shock or corner. Downstream of this point the pressure gradients become quite steep again, whereas with the original functions the pressure gradients are much smaller here. Experimentally it would be difficult to obtain an entirely laminar interaction with the same sort of Reynolds number at separation and such an extensive region of separation as in Fig.6. However for more modest regions of separation, the shape of the pressure distribution as predicted using the lower-branch functions of Table 1 is in better agreement with experiment than that obtained using the original functions. The latter give rise to pressure gradients in the vicinity of reattachment that are much too small relative to those in the vicinity of separation.

The pressure gradient changes abruptly at the shock or corner according to the lower-branch parameters, but remains continuous according to the original ones. Experimental results[5,13,14,15] show that there is no discontinuous change, but there is a fairly rapid change of gradient if the thickness of the region of reversed flow near the wall is not too great a proportion of the total boundary-layer thickness. The theoretical change of gradient is due to the term $K'E$ in the numerator of equation (26) for $dw/d\zeta$. E decreases discontinuously at the shock or corner, where $\bar{w}$ changes from w_o to w_∞, so that ϕ changes from positive to negative. Hence since K'^o is positive for the lower-branch functions in a region of separation, $dw/d\zeta$ decreases abruptly and the pressure gradient correspondingly increases. For the original functions K' is zero so that the gradient remains continuous. In physical terms the rates of change of the shapes of the velocity and temperature profiles change abruptly

at/

at the shock or corner, and for the lower-branch parameters this means a discontinuous change in dI/dx, the gradient of the momentum flux in the boundary layer, and a corresponding change in the pressure gradient.

Figs.8 to 11 show results for Cases 3 and 4, which are at a Mach number M_o of 3 and a Reynolds number at separation of about 0.5×10^6. Case 3 is for incipient separation, and Case 4 is with $w_\infty = 1.71$, corresponding to a change in wall slope in Fig.2 of about 7°. These results are shown in some detail because they are used as the basis of comparison with various other cases, discussed below. It will be noticed that the displacement thickness changes much more violently in proportion than the momentum thickness. This is because the outer part of the velocity profile tends to maintain a roughly constant shape, as observed experimentally.[13,14] The momentum thickness depends mainly on the outer part of the profile, the region of low-velocity air near the surface usually only making a small contribution to it. The displacement thickness, on the other hand, is very much affected by the low-velocity region, which becomes thick in the separated region, and reaches a maximum thickness at the position of the shock or corner.

Detailed comparison with experiment is not easy because the available data[5,13,14,15] for entirely laminar interactions do not correspond exactly to the cases worked out here. However, as regards the order of magnitude of the upstream influence, pressure rise to separation, etc., the theoretical results seem to agree with experiment.

Fig.12 shows the results for Case 4 compared with those for Case 5, which is for the same conditions, but calculated according to the parameters of Table 3 rather than Table 1. Table 3 is based on the 0.98 definition of the edge of the boundary layer, whereas Table 1 is based on the usual 0.95 value. It can be seen that the two curves agree quite well in general shape, but upstream of separation the predicted pressure gradients are considerably steeper for the 0.98 definition than for the normal one. The biggest differences in the pressure gradients would be expected to occur here for two reasons. In the first place, the inclusion of rather more supersonic flow in the boundary layer, involved in the 0.98 definition, is probably more important where the layer is attached than where it is separated. This is because the separated layer has a large region of slow-moving fluid, and the expansion of these low-speed stream tubes in an adverse pressure gradient will swamp any effects due to the contraction of the supersonic stream tubes. The second reason is that all definitions of the edge of the layer would give the correct answers, and hence agree with each other, if they all happened to require the pressure distribution acting on the boundary layer to be of the same form, a form leading to similar profiles. Fig.13 shows that for the results of Case 4 the factor β, equal to $2n/(n+1)$, where n is the index of the equivalent low-speed power-law velocity distribution, varies much more rapidly upstream of separation than downstream of it. Thus, downstream of separation the pressure distribution seems to be closer to that required to give similar profiles, and better agreement between the two sets of results might be expected. These considerations, and the results of Fig.12, are an encouraging indication that the arbitrariness in the definition of the edge need not in practice lead to serious errors.

Fig.14 shows a comparison of the results of Cases 3 and 6. The latter case is for the same conditions as Case 3, but C in the table of parameters has been arbitrarily doubled. C is proportional to the entrainment of fluid from the mainstream into the boundary layer, and Fig.14 verifies that this is indeed a significant physical process, since the results are considerably dependent on the magnitude of C, the pressure coefficient at separation, for example, being increased by about 23% by doubling C. (It had been suggested that the results might be insensitive to C).

Fig.15/

Fig.15 shows in the full-line curve the result for Case 3 again. Compared with this is the result for Case 7, the incipient separation of a boundary layer at the same Mach number and approximately the same Reynolds number at separation, but with a cooled wall, whose absolute temperature is maintained at 0.6 times the stagnation temperature of the mainstream. It requires a somewhat higher pressure to cause separation in the cooled layer. Also the upstream influence is less, the pressure gradients upstream of separation being somewhat steeper with cooling. Experimental observations[16,17] show little effect of heat transfer on the pressure gradients. The thickness of the boundary layer is reduced by cooling, the displacement thickness of the cooled layer just upstream of the region of interaction being about 2/3 that of the layer with zero heat transfer.

A similar comparison is shown in Fig.16 for the results of Cases 4 and 8, though here the overall pressure ratio is specified such that $w_\infty = 1.71$. This corresponds to a change of wall slope in Fig.2 of about 7°. The upstream effect is greatly reduced by cooling, by a much greater proportion than the proportional reduction in the displacement thickness of the upstream boundary layer. No experimental data are available to check this conclusion: the data[16,17] mentioned above, in connection with the pressure gradients at separation, are for cases where the boundary layer is laminar at separation but turns turbulent before reattachment, whereas the present calculations assume entirely laminar flow. They are thus not comparable as regards the magnitude of the upstream effect, a point discussed further below.

Suction has a similar effect to cooling, as can be seen from Figs.17 and 18, showing Case 9 compared with Case 3 and Case 10 with Case 4. The suction cases, shown in the dotted curves, are calculated with the suction parameter G of the basic similar profiles equal to 0.4. Thus they correspond roughly, according to equation (37), to cases with uniform suction with a suction coefficient between 0.0004 and 0.0008. It can be seen that, as it happens, the pressure distribution with this particular rate of suction in Fig.18 is almost the same as that with the particular degree of wall cooling in Fig.16. The displacement thickness of the boundary layer with suction just upstream of the region of interaction is about 73% of the value for the corresponding case without suction. The predicted effect of suction on the pressure distribution is in qualitative accord with experiment[14].

The remaining cases calculated can be disposed of briefly. Fig.19 shows results for Cases 11 and 12, the same as Cases 3 and 4 except that the Reynolds number is lower. It can be seen by comparison with Fig.8 that due to the lower Reynolds number the pressure at separation is higher, and the upstream effect for a given overall pressure ratio is less. These effects of Reynolds number are observed experimentally[5,15]. The overall shape of the pressure distribution calculated for Case 12 is much more typical of the shapes obtained experimentally than is the predicted shape for Case 4. It would not be easy to obtain experimentally a laminar interaction under the conditions of Case 4, because of the relatively high Reynolds number and overall pressure rise.

Figs.20 to 22 show results of Cases 13 to 17 for the "laminar foot" at various Reynolds numbers, both with zero heat transfer and with the wall cooled to 0.6 times the stagnation temperature of the mainstream. The laminar foot[5] corresponds to that part of the pressure-distribution curve upstream of the shock or corner and also upstream of transition, if this occurs within the region of interaction. It is easier to obtain experimentally interactions which are laminar at separation but turn turbulent before reattachment, rather than entirely laminar ones. The shape of the laminar foot is thus of considerable practical interest. If transition occurs, the position of the shock (Fig.1) or corner (Fig.2) relative to separation cannot be predicted as a function of the overall pressure rise. However the predicted shape of the laminar foot, calculated as far as some arbitrarily specified position downstream of separation, can

be/

be compared with experiment, as far as the foot extends in any particular experimental case. Such a comparison[5,13,15,16,17] with Figs.20 to 22 shows that whilst the theory is qualitatively all right at the lower Reynolds numbers, though predicting rather too large an effect of wall temperature on the pressure distribution, it becomes increasingly unsatisfactory in well-separated regions at high Reynolds numbers, where it predicts a strongly falling pressure downstream of a pressure maximum on the laminar foot. This effect is accentuated by cooling the wall. In reality the laminar foot has a level plateau region, provided the wall is flat as assumed in the present calculations. If the original type of parameters had been used, the pressure gradients would have remained positive, but would not have fallen off as sharply downstream of separation as they do in reality, so that the plateau region would have been much too high. The predicted pressure maximum in Figs.20 to 22 is at about the same level as the experimental plateau pressure[5,15] and decreases with increasing Reynolds number in a similar way.

Finally, Fig.23 shows a further example with suction, Case 19, compared with the corresponding Case 18 without suction. The upstream Mach number is 1.4, the Reynolds number at separation is about 0.5×10^6, and the conditions are for incipient separation. The suction parameter G is again 0.4 so that, by equation (37), the case is roughly equivalent to one with uniform suction with a suction coefficient of between 0.0004 and 0.0008. Qualitatively the results are similar to those of Fig.17, at a higher Mach number.

8. Comparison with Other Methods

The Crocco-Lees method gives results that are qualitatively reasonable in many respects for interactions between shock waves and entirely laminar boundary layers, including effects of heat transfer and suction. Once the method has been programmed for automatic computation on a computer such as the N.P.L. DEUCE, its application is reasonably speedy. However the algebraic complexity of the method makes the programming a difficult matter, and it was a long time before all the difficulties and snags were sorted out in the present work. Therefore, since the results are still of only qualitative validity, the question arises as to whether there may be other approximate methods, not dependent on automatic computation, which might be better for general application. Hitherto the available alternative methods have been more restricted in scope, being limited, for example, to cases with little separation or with no heat transfer or suction. Thus Stratford's method[18], as modified by Gadd[19] for use in cases with compressible flow, ceases to work satisfactorily much beyond separation. However it gives results comparable to those given by the Crocco-Lees method for the effect of heat transfer on the shape of the pressure distribution in the vicinity of separation. Fig.24 shows such a comparison for the cases shown in Fig.21. It can be seen that the Stratford-Gadd method predicts a marked effect of wall temperature on the pressure gradient, the predicted variation being as $T_w^{-3/2}$, where T_w is the absolute temperature of the wall. This is a larger variation than is predicted by the Crocco-Lees method, so that since experiment[16,17] shows little effect of wall temperature on the shape of the pressure distribution, the Stratford-Gadd theory is worse than that of Crocco-and Lees in this respect. It appears, however, to give rather more accurate results for the pressure rise to separation in cases with zero heat transfer. The pressure coefficient $2(p - p_o)/\rho_o u_o^2$ at separation is predicted to be given by the simple formula $1.13(M_o^2 - 1)^{\frac{1}{4}} R_{xs}^{-\frac{1}{4}}$, and according to the experimental results of Ref.13 for zero heat transfer, it is equal to $0.93(M_o^2 - 1)^{-\frac{1}{4}} R_{xs}^{-\frac{1}{4}}$ approximately.

A simple new method which, like that of Crocco and Lees, is applicable to cases with extensive separation, can be developed on the lines

of/

of the well-known Pohlhausen method for incompressible flow, and is closely related to the methods of Refs. 14,20,21 and 22. In its simplest form it is as follows:

$$\text{Put} \qquad \frac{u}{u_e} = f(\lambda), \qquad \lambda = \int_0^y \frac{\rho}{\rho_e}\, dy. \qquad \ldots (38)$$

Then the displacement and momentum thickness are

$$\delta^* = \int_0^\infty \left(\frac{T}{T_e} - \frac{u}{u_e} \right) d\lambda$$

and

$$\theta = \int_0^\infty \frac{u}{u_e}\left(1 - \frac{u}{u_e}\right) d\lambda.$$

But by definition,

$$\left(C_p T + \frac{u^2}{2}\right) \Big/ \left(C_p T_e + \frac{u_e^2}{2}\right) = H,$$

the total-temperature ratio. Hence

$$\frac{T}{T_e} = \left(1 + \frac{\gamma - 1}{2} M_e^2\right) H - \frac{\gamma - 1}{2} M_e^2 \frac{u^2}{u_e^2} \qquad \ldots (39)$$

and

$$\frac{\delta^*}{\theta} = \left(1 + \frac{\gamma - 1}{2} M_e^2\right) r_1 + \frac{\gamma - 1}{2} M_e^2, \qquad \ldots (40)$$

where

$$r_1 = \int_0^\infty \left(H - \frac{u}{u_e}\right) d\lambda \Big/ \int_0^\infty \frac{u}{u_e}\left(1 - \frac{u}{u_e}\right) d\lambda . \qquad \ldots (41)$$

As an alternative to (39), we may assume that approximately

$$\frac{T}{T_e} = 1 + \frac{\gamma - 1}{2} M_e^2 \left(\frac{u}{u_e} - \frac{u^2}{u_e^2} \right) + \left(\frac{T_w}{T_e} - 1 \right)\left(1 - \frac{u}{u_e}\right) . \qquad \ldots (42)$$

If the Prandtl number is 1, this approximation is accurate upstream of the region of interaction, where the pressure gradient is zero, but it is not accurate elsewhere unless there is zero heat transfer. However its use slightly simplifies the analysis, as will be seen below. According to relation (42)

$$\frac{\delta^*}{\theta} = \frac{T_w}{T_e} r_2 + \frac{\gamma - 1}{2} M_e^2 \qquad \ldots (43)$$

where

$$r_2 = \int_0^\infty \left(1 - \frac{u}{u_e}\right) d\lambda \Big/ \int_0^\infty \frac{u}{u_e}\left(1 - \frac{u}{u_e}\right) d\lambda . \qquad \ldots (44)$$

In cases without heat transfer $r_1 = r_2$, and (40) is the same as (43).

If/

If viscosity is proportional to absolute temperature it follows from equations (38) and the momentum equation,

$$\rho u \frac{\partial u}{\partial x} + \rho v \frac{\partial u}{\partial y} = - \frac{dp}{dx} + \frac{\partial}{\partial y}\left(\mu \frac{\partial u}{\partial y}\right),$$

that at the wall

$$\frac{dp}{dx} = \frac{\mu_e u_e}{\theta^2} \frac{T_e}{T_w}\left[\left(\frac{\partial^2 f}{\partial \ell^2}\right)_w + N\left(\frac{\partial f}{\partial \ell}\right)_w\right], \qquad \ldots (45)$$

where $\ell = \lambda/\theta$ and $N = \rho_e u_e \theta C_Q/\mu_e = - \rho_w v_w \theta/\mu_e$. Also, from a first-order approximation to the simple-wave-flow relation,

$$\frac{dp}{dx} = \frac{\rho_o u_o^2}{(M_o^2 - 1)^{\frac{1}{2}}} \frac{d^2\delta^*}{dx^2}. \qquad \ldots (46)$$

We assume that M_e and θ in equations (40) and (43) are virtually constant through the region of interaction. Typically M_e does not differ very greatly from M_o since it is impossible to have an entirely laminar interaction with a large pressure rise, unless the Reynolds number R_{xs} at separation is very low. With regard to θ, inspection of the von Kármán momentum integral equation, i.e.,

$$\frac{d\theta}{dx} + \frac{1}{u_e}\frac{du_e}{dx}(2\theta + \delta^*) + \frac{\theta}{\rho_e}\frac{d\rho_e}{dx} = \frac{\tau_w}{\rho_e u_e^2} - C_Q, \qquad \ldots (47)$$

suggests that $\frac{d\theta}{dx}$ is unlikely to be much greater within the interaction region than it is upstream of it. Hence if the length of the interaction region is not too large a fraction of the distance from, say, the separation point to the leading edge, θ should not change enormously through the region of interaction. Experiment[13,14] confirms this. So also does Fig.11, a case calculated by the Crocco-Lees method, even though for this case the extent of the separated region is quite large (larger than could easily be obtained experimentally). We accordingly substitute for θ in equations (40) and (43) the constant value θ_s as determined from the momentum integral equation (47) with u_e, μ_e, and ρ_e set constant at the values u_o, μ_o, and ρ_o corresponding to free-stream flow parallel to the wall upstream of the region of interaction, and with x put equal to x_s, the distance of the separation point from the leading edge. The equation becomes

$$\frac{d\theta}{dx} = \frac{\mu_o}{\rho_o u_o \theta}\left[\left(\frac{\partial f}{\partial \ell}\right)_{wc} - N\right]$$

where $(\partial f/\partial \ell)_{wc}$ is the value of $(\partial f/\partial \ell)$ at the wall at constant pressure. Hence

$$\theta_s = 2^{\frac{1}{2}}\left[\left(\frac{\partial f}{\partial \ell}\right)_{wc} - N\right]^{\frac{1}{2}} \frac{x_s}{R_{xs}^{\frac{1}{2}}}, \qquad \ldots (48)$$

if/

if N is assumed to be constant. This assumption is equivalent to making the suction parameter G constant in the Crocco-Lees analysis. Thus it follows from equation (36) that

$$\frac{N}{\left[\left(\frac{\partial f}{\partial \ell}\right)_{wc} - N\right]^{\frac{1}{2}}} = G. \qquad \ldots (49)$$

From equations (40), (43), (45) and (46),

$$\frac{d^2 r}{dx^2} = \frac{T_o^2 (M_o^2 - 1)^{\frac{1}{2}} x_s}{T_w^2 A^2 \theta_s^3 R_{xs}} \left[\left(\frac{\partial^2 f}{\partial \ell^2}\right)_w + N\left(\frac{\partial f}{\partial \ell}\right)_w\right],$$

where if equation (40) is used $r = r_1$ and

$A = \left(1 + \frac{\gamma-1}{2} M_o^2\right)^{\frac{1}{2}} T_o^{\frac{1}{2}} \Big/ T_w^{\frac{1}{2}} = H_w^{-\frac{1}{2}}$, and if equation (43) is used, $r = r_2$ and $A = 1$. We assume that $\left(\frac{\partial^2 f}{\partial \ell^2}\right)_w$ and $\left(\frac{\partial f}{\partial \ell}\right)_w$ are functions only of r for a given value of N and a given ratio H_w of the wall temperature to the free-stream stagnation temperature. Hence

$$\frac{dr}{dx} = \pm 2^{\frac{1}{2}} \frac{T_o}{T_w A} \frac{(M_o^2 - 1)^{\frac{1}{4}} x_s^{\frac{1}{2}} Q^{\frac{1}{2}}}{\theta_s^{\frac{3}{2}} R_{xs}^{\frac{1}{2}}} \qquad \ldots (50)$$

where $$Q \equiv \int_{r_c}^{r} \left[\left(\frac{\partial^2 f}{\partial \ell^2}\right)_w + N\left(\frac{\partial f}{\partial \ell}\right)_w\right] dr,$$

and r_c is the value of r at constant pressure. Upstream of the shock in Fig.1 or corner in Fig.2 δ^* increases with x, and hence the positive sign must be taken in (50), but downstream δ^* decreases, and the negative sign must be used. From equations (46) and (48) it follows that upstream

$$\frac{p - p_o}{p_o} = \frac{2^{\frac{1}{4}} \gamma M_o^2 A Q^{\frac{1}{2}}}{(M_o^2 - 1)^{\frac{1}{4}} R_{xs}^{\frac{1}{4}} \left[\left(\frac{\partial f}{\partial \ell}\right)_{wc} - N\right]^{\frac{1}{4}}} \qquad \ldots (51)$$

and downstream

$$\frac{p_\infty - p}{p_o} = \frac{2^{\frac{1}{4}} \gamma M_o^2 A Q^{\frac{1}{2}}}{(M_o^2 - 1)^{\frac{1}{4}} R_{xs}^{\frac{1}{4}} \left[\left(\frac{\partial f}{\partial \ell}\right)_{wc} - N\right]^{\frac{1}{4}}}.$$

Thus the shock or corner must occur at that position where $p = \frac{1}{2}(p_o + p_\infty)$, i.e., where the pressure rise is half the overall pressure rise. The shape of the pressure distribution is symmetrical about this point, reflected in the two axes of symmetry as shown in Fig.25. Upstream of the shock or corner it follows from (50) that

$$\frac{x - x_s}{x_s} /$$

$$\frac{x - x_s}{x_s} = 2^{\frac{1}{4}} \frac{T_w A}{T_o} \frac{\left[\left(\frac{\partial f}{\partial \ell}\right)_{wc} - N\right]^{\frac{3}{4}}}{(M_o^2 - 1)^{\frac{1}{4}} R_{xs}^{\frac{1}{4}}} \int_{r_s}^{r} \frac{dr}{Q^{\frac{1}{2}}}, \qquad \ldots (52)$$

where r_s is the value of r at separation. Equations (51) and (52) determine the shape of the pressure distribution.

This solution could of course be regarded merely as a first approximation, from which more accurate solutions of equations (45), (46), and (47) could be obtained by iteration. However this would be laborious. It might be thought that some converse process of simplification could be applied to the Crocco-Lees method, reducing it to a single equation from which results could be obtained simply, without necessarily using automatic computing aids. However this does not appear to be possible except for cases with very large Reynolds numbers.[7]

Due to the approximation made in the present Pohlhausen-type of method that θ is constant, the small rate of thickening of the boundary layer upstream of the shock is neglected. Hence, as can be seen from equation (51), the pressure upstream is predicted to tend to p_o, instead of to a value a little greater than p_o, as in equation (32) of the Crocco-Lees method.

The relations between the parameters involved in (51) and (52), namely $\left(\frac{\partial^2 f}{\partial \ell^2}\right)_w$, $\left(\frac{\partial f}{\partial \ell}\right)_w$ and r, can be obtained from the similarity solutions. If there is no suction, so that N is zero, then upstream of the region of interaction, f as a function of ℓ is independent of heat transfer, and r_2 is similarly independent, so that $\left(\frac{\partial f}{\partial \ell}\right)_{wc}$ and r_{2c} are constants, 0.221 and 2.59 respectively. As an approximation we can assume that everywhere f is a function only of ℓ and r_2, independent of heat transfer. Thus Q as a function of r_2 is assumed to be independent of wall temperature, and can accordingly be determined from the similarity solutions for zero heat transfer. Then since $A = 1$ if equation (42) is used, it can be seen from (51) and (52) that the only effect of heat transfer on the shape of the pressure distribution is to stretch the x-co-ordinates proportionally to T_w, so that the pressure gradient varies as T_w^{-1}. As mentioned above the Stratford-Gadd theory predicts a variation as $T_w^{-\frac{3}{2}}$. Even the variation as T_w^{-1} is considerably larger than is observed experimentally.

We shall refer to the above method of solution as method A for heat transfer. A second, theoretically preferable, method, method B, involves the use of the accurate temperature relation (39). Then r must be put equal to r_1, and the relation between $\left(\frac{\partial^2 f}{\partial \ell^2}\right)_w$ and r must be found from the similarity solutions corresponding to the particular value of H_w for the case being investigated. The predicted effect of heat transfer on the shape of the pressure distribution is accordingly less simple than that found by method A.

In/

In cases without heat transfer, $r_1 = r_2 = r$, even if there is suction. Q as a function of r, r_c and $\left(\frac{\partial f}{\partial \ell}\right)_{wc}$ can be found from the similarity solution with zero heat transfer but with the suction appropriate to the particular value of N, which gives G by equation (49). This procedure may be described as method B for suction cases. It may, however, be more convenient to use what we term method A, in which it is assumed that the family of velocity profiles is the same as that calculated from the similar solutions without suction. Then, in virtue of condition (45), r_c and $\left(\frac{\partial f}{\partial \ell}\right)_{wc}$ are the values of r and $\left(\frac{\partial f}{\partial \ell}\right)_{w}$ corresponding to the profile for which $\left(\frac{\partial^2 f}{\partial \ell^2}\right)_w + N\left(\frac{\partial f}{\partial \ell}\right)_w = 0$. This equivalent zero-pressure-gradient profile with suction will actually be a profile without suction, but with a favourable pressure gradient. By this artifice it is possible to obtain approximate solutions for cases with suction, without first solving the accurate similarity solutions for the particular value of N being considered*. However, both with method A and with method B, equations (51) and (52) show that the pressure distribution is not related to the corresponding one without suction by any simple stretching of the co-ordinates. Thus the solutions with suction are not quite so simple as the method A solutions with heat transfer.

The relations between the parameters r, $\left(\frac{\partial f}{\partial \ell}\right)_w$ and $\left(\frac{\partial^2 f}{\partial \ell^2}\right)_w$, as derived from the similarity solutions for zero heat transfer and suction, are presented in Table 6. This is applicable not only to cases without heat transfer or suction, but generally, in the method A approximation For the case with suction at $G = 0.4$, the equivalent constant-pressure conditions are $r_c = 2.36$, $\left(\frac{\partial f}{\partial \ell}\right)_{wc} = 0.302$, and $\left(\frac{\partial^2 f}{\partial \ell^2}\right)_{wc} = -0.0465$. According to the actual similarity solutions with suction the values are 2.39, 0.290 and -0.0432 respectively, so that the errors are not large. In other words, the true-constant pressure velocity profile with suction is very similar to the profile without suction but with the appropriate favourable pressure gradient.

Although the similar solutions with suction with $G = 0.4$ have been worked out in connection with the Crocco-Lees parameters, the present application was unfortunately not foreseen, so that for method B with suction some of the data necessary for the calculation of r, $\left(\frac{\partial f}{\partial \ell}\right)_w$, and $\left(\frac{\partial^2 f}{\partial \ell^2}\right)_w$, are not readily available. Hence in the present paper cases with suction can only be calculated by method A, and not by method B. For cases with heat transfer with $H_w = 0.6$, however, both method A and method B can be used, since Cohen and Reshotko[12,21] give sufficient data for the calculation of the parameters which are given in Table 7. As was the case with the Crocco-Lees parameters, some interpolation between the results for different rates of heat transfer was necessary to obtain the lower-branch values beyond separation.

The calculated results for $Q^{\frac{1}{2}}$ and $\int_{r_s}^{r} \frac{dr}{Q^{\frac{1}{2}}}$, the main quantities to be determined in equations (51) and (52), are shown in Tables 8 to 10 as

functions/

---

*A similar procedure can of course be used to obtain the Crocco-Lees parameters for cases with suction, and was so used in Ref.3.

functions of $r - r_c$. From these tables it is possible to calculate rapidly a wide variety of cases with different Reynolds numbers and Mach numbers. Sample calculated results for the laminar foot are shown in Figs.26 and 27. The cases shown are all for a free-stream Mach number of 3 and Reynolds number R_{xs} at separation of 0.5×10^6. They are thus comparable with Figs.16 and 18. The predicted effect of heat transfer in Fig.26 is, according to method A, simply to vary the pressure gradients proportionally to T_w^{-1} as mentioned above. According to method B heat transfer has a smaller effect on the pressure gradients, but the pressure rise to separation is somewhat increased by cooling. Thus method B is more in line with the predictions of the Crocco-Lees method than is method A. Also, since method B predicts a smaller effect on the overall shape of the pressure distribution than method A, it is less discordant with experiment. For cases with suction, the effects shown in Fig.27 are broadly similar to those found by the Crocco-Lees method in Fig.18.

The predicted pressure coefficient at separation with zero heat transfer or suction (or with heat transfer according to method A), is equal to $0.94\,(M_o^2 - 1)^{-\frac{1}{4}} R_{xs}^{-\frac{1}{4}}$, almost exactly in agreement with the experimental results of Ref.13. These data, (which may be subject to inaccuracies due to the practical difficulties of determining the precise position of separation), show that the pressure rise to separation is slightly more than half that to the plateau at the top of the laminar foot. This ratio is rather bigger than that given by the present Pohlhausen-type of method, and considerably smaller than that predicted by the Crocco-Lees method, especially at high Reynolds numbers.

According to the results of Figs.26 and 27 the plateau pressure with zero heat transfer or suction is about 1.34 times the upstream pressure. Thus the overall pressure ratio cannot exceed about 1.68. This happens to be approximately equal to the pressure ratio assumed for the Crocco-Lees calculations of Figs.16 and 18. Thus the present Pohlhausen-type of method would predict a very large upstream effect for this pressure ratio, and for any larger ratio it would predict that the separation point must move right forward to the leading edge. This prediction cannot readily be checked experimentally because in practice as the pressure ratio is increased there comes a point where transition to turbulent flow takes place within the region of interaction, and the theories no longer apply. Thus transition would very likely occur in practice before the conditions of Figs.16 and 18 could be attained. For a smaller specified overall pressure ratio it is clear from Figs.25, 26 and 27 that cooling and suction would reduce the upstream effect of the interaction, just as they do according to the Crocco-Lees method.

9. Concluding Remarks

The results of the Crocco-Lees method, although in general qualitative agreement with experiment, are probably no better than those obtained much more readily by a Pohlhausen type of method. Thus there seems little point in doing any further calculations by the Crocco-Lees method. However, what has been done has probably been worthwhile since it justifies the approximations of the Pohlhausen-type of method presented in Section 8, and it is always desirable to check the findings of different approximate methods against each other as well as against experiment, where this is possible.

The main qualitative results of the approximate theories now available for interactions between shocks and laminar layers are as follows:

(1)/

(1) The general shape of the pressure distribution, and the pressure levels, are predicted satisfactorily on the whole, though in some cases the results become unrealistic beyond a little way downstream of separation. Lowering the Reynolds number is found to increase the pressure rise to separation and to decrease the upstream influence if the overall pressure rise (related to the incident shock strength in Fig.1 or change of wall slope in Fig.2) is specified. This is qualitatively in accord with experiment.

(2) Cooling the wall, according to some theories, greatly increases the pressure gradients in the vicinity of separation, leaving the pressure at separation unchanged, but according to others, the pressure rise to separation is somewhat increased whilst there is only a modest steepening effect on the gradients. All the theories predict a bigger effect on the overall shape of the distribution than is observed experimentally. The upstream effect for a given overall pressure ratio is predicted to be reduced by cooling. There is no experimental evidence on this point to date.

(3) Suction is predicted to have a qualitatively similar effect to wall cooling. This appears to be confirmed by the available experimental data.

Acknowledgments

The computations of the similar solutions with suction were carried out by Mr. A. R. Curtis of the Mathematics Division, N.P.L., and the computations involved in Section 8 were performed by Mrs. B. Howard and Miss R. Warren of the Aerodynamics Division, N.P.L.

List of Symbols

A constant equal either to $\left(1 + \frac{\gamma - 1}{2} M_o^2\right)^{\frac{1}{2}} T_o^{\frac{1}{2}}/T_w^{\frac{1}{2}} = H_w^{-\frac{1}{2}}$, or to 1

a speed of sound

B $(1 - K)(1 - \sigma) + C_Q/C_M$

C mC_M/μ_e, one of the basic Crocco-Lees parameters

C_f coefficient of local skin friction, $2\tau_w/\rho_e u_e^2$

C_M mixing rate coefficient, $d\delta/dx - \phi + \rho_w v_w/\rho_e u_e$

C_p specific heat at constant pressure

C_Q suction coefficient, $- \rho_w v_w/\rho_e u_e$

E $t\phi/C_M + t\sigma(1 - K) - \psi$

F non-dimensional stream function for similar solutions: see equation (20)

f u/u_e

G suction parameter for similar solutions: see equation (20)

H/

H ratio of total temperature to its value in the free stream

I momentum flux, $\int_0^\delta \rho u^2 \, dy$

J $\gamma w^2 \psi + Kt(w^2 - t)$

ℓ λ/θ

M Mach number

m mass flux, $\int_0^\delta \rho u \, dy$

N $\rho_e u_e \theta C_Q / \mu_e$

n index of similar-solutions power-law velocity distribution: see equation (20)

P p/p°

p pressure

Q integral defined in equation (50)

R_x Reynolds number based on x, $\rho_o u_o x/\mu_o$

R_{δ^*} Reynolds number based on displacement thickness, $\rho_o u_o \delta^*/\mu_o$

R_θ Reynolds number based on momentum thickness, $\rho_o u_o \theta/\mu_o$

r equal to r_1 or r_2

r_1 $\int_0^\infty \left(H - \frac{u}{u_e}\right) d\lambda \Big/ \int_0^\infty \frac{u}{u_e}\left(1 - \frac{u}{u_e}\right) d\lambda$

r_2 $\int_0^\infty \left(1 - \frac{u}{u_e}\right) d\lambda \Big/ \int_0^\infty \frac{u}{u_e}\left(1 - \frac{u}{u_e}\right) d\lambda$

s stream function in Stewartson transformation: see equation (17)

T absolute temperature

t ratio of the temperature at the edge of the boundary layer to the free-stream stagnation temperature

u velocity component parallel to wall

v velocity component normal to wall

w u_e/a°

X $(x - x_s)/\delta_s$

x distance from leading edge measured parallel to wall

$\bar{x}$ related to x by the Stewartson transformation, equation (17)

y/

y distance from wall measured normal to wall

$\bar{y}$ related to y by the Stewartson transformation, equation (17)

β $2n/(n + 1)$

γ ratio of specific heat at constant pressure to that at constant volume: assumed to equal 1.4

Δ δ/δ_s

δ total thickness of boundary layer

δ^* displacement thickness of boundary layer, $\int_o^\infty \left(1 - \frac{\rho u}{\rho_e u_e}\right) dy$

ζ m/μ^o

η non-dimensional co-ordinate for similar solutions: see equation (20)

θ momentum thickness of boundary layer, $\int_o^\infty \frac{\rho u}{\rho_e u_e}\left(1 - \frac{u}{u_e}\right) dy$

K I/Mu_e, one of the basic Crocco-Lees parameters

λ $\int_o^y \frac{\rho}{\rho_e} dy$

μ viscosity

ρ density

σ $mC_f/2(1 - K)C\mu_e$, one of the basic Crocco-Lees parameters

τ viscous shear stress

ϕ angle between the wall and the streamlines at the edge of the boundary layer

ψ $t[(\rho_e u_e \delta/m) - K]$, one of the basic Crocco-Lees parameters

Suffices:

c denotes values of the boundary-layer parameters for constant-pressure conditions

e denotes conditions at the edge of the boundary layer

w denotes conditions at the wall

s denotes conditions at the separation point

o denotes conditions in the free stream for flow parallel to the wall upstream of the shock or corner

∞ denotes conditions in the free stream for flow parallel to the wall downstream of the shock or corner

Superscript:

o denotes free-stream stagnation conditions

References/

References

No.	Author(s)	Title, etc.
1	Crocco, L. and Lees, L.	A mixing theory for the interaction between dissipative flows and nearly isentropic streams. J. Aero. Sci., Vol.19, p.649, 1952.
2	Crocco, L.	Considerations on the shock wave boundary layer interaction. Proceedings of the Centenary Meeting of Brooklyn Polytechnic Institute, p.75, December, 1954.
3	Bray, K. N. C.	Some notes on shock-wave boundary-layer interactions, and on the effect of suction on the separation of laminar boundary layers. A.R.C. C.P.332, August, 1956.
4	Bray, K. N. C.	The effect of heat transfer on interactions involving laminar boundary layers. A.R.C. C.P.339, August, 1956.
5	Gadd, G. E., Holder, D. W. and Regan, J. D.	An experimental investigation of the interaction between shock waves and boundary layers. Proc. Roy. Soc. A., Vol.226, p.227, 1954.
6	Stewartson, K.	Correlated incompressible and compressible boundary layers. Proc. Roy. Soc. A, Vol.200, p.84, 1949.
7	Bray, K. N. C.	The application of the theory of Crocco and Lees to shock boundary-layer interactions. Princeton University Aero. Eng. Report 322, July, 1955. A.R.C.18,432 - F.M.2401. May, 1956.
8	Cheng, Sin-I. and Chang, I. D.	On the mixing theory of Crocco and Lees and its application to the interaction of shock wave and laminar boundary layer. Part II. Results and discussion. Princeton University Aero. Eng. Report 376, November, 1957. P.73998.
9	Stewartson, K.	Further solutions of the Falkner-Skan equation. Proc. Camb. Phil. Soc., Vol.50, p.454, 1954.
10	Lighthill, M. J.	On boundary layers and upstream influence. Part II. Supersonic flows without separation. Proc. Roy. Soc. A, Vol.217, p.478, 1953.
11	Hartree, D. R.	On an equation occurring in Falkner and Skan's approximate treatment of the equations of the boundary layer. Proc.Camb. Phil. Soc., Vol.33, p.223, 1937.
12	Cohen, C. B. and Reshotko, E.	Similar solutions for the compressible laminar boundary layer with heat transfer and pressure gradient. N.A.C.A. Report 1293, 1956.
13	Hakkinen, J., Greber, I., Trilling, L. and Abarbanel, S. S.	The interaction of an oblique shock wave with a laminar boundary layer. N.A.S.A. Memo.2-18-59W, March, 1959. TIL6276.
14	Greber, I.	Interaction of oblique shock waves with laminar boundary layers. Fluid Dynamics Research Group, Massachusetts Institute of Technology, Technical Report 59-2, April, 1959. P.89944.

15/

No.	Author(s)	Title, etc.
15	Chapman, D. R., Kuehn, D. M. and Larson, H. K.	Investigation of separated flows in supersonic and subsonic streams, with emphasis on the effect of transition. N.A.C.A. Report 1356, 1958.
16	Gadd, G. E.	An experimental investigation of heat transfer effects on boundary layer separation in supersonic flow. J. Fluid Mech., Vol.2, p.105, 1957.
17	Gadd, G. E. and Holder, D. W.	The behaviour of supersonic boundary layers in the presence of shock waves. Paper presented at the seventh Anglo-American Aeronautical Conference, New York, October, 1959.
18	Stratford, B. S.	Flow in the laminar boundary layer near separation. A.R.C. R. & M.3002, November, 1954.
19	Gadd, G. E.	A theoretical investigation of laminar separation in supersonic flow. J. Aero. Sci., Vol.24, p.759, 1957.
20	Gadd, G. E.	A simple theory for interactions between shock waves and entirely laminar boundary layers. J. Aero. Sci., Vol.23, p.225, 1956.
21	Cohen, C. B. and Reshotko, E.	The compressible laminar boundary layer with heat transfer and arbitrary pressure gradient. N.A.C.A. Report 1294, 1956.
22	Curle, S. N.	Paper in preparation.

Table 1/

Table 1

Crocco-Lees parameters for zero heat transfer or suction, with usual edge definition

ψ	K	K'	C	σ	Remarks
1.033	0.704 95	- 0.1440	2.240	1.350	
1.083	0.698 60	- 0.1172	2.420	1.002	Constant pressure
1.133	0.693 23	- 0.1050	2.579	0.789	
1.183	0.688 10	- 0.1025	2.700	0.641	
1.233	0.682 97	- 0.0952	2.770	0.523	
1.283	0.678 58	- 0.0830	2.830	0.430	
1.333	0.674 67	- 0.0732	2.885	0.350	
1.383	0.671 25	- 0.0586	2.930	0.275	
1.433	0.668 81	- 0.0415	2.965	0.211	
1.483	0.667 10	- 0.0293	2.990	0.158	
1.533	0.665 88	- 0.0220	3.008	0.109	
1.583	0.664 91	- 0.0146	3.020	0.068	
1.633	0.664 42	- 0.0049	3.030	0.033	
1.683	0.664 42	0	3.040	0	Separation
1.733	0.664 42	0	3.040	- 0.029	
1.783	0.664 42	+ 0.0024	3.030	- 0.051	
1.833	0.664 66	0.0073	3.015	- 0.070	
1.883	0.665 15	0.0146	3.000	- 0.090	
1.933	0.666 13	0.0244	2.984	- 0.111	
1.983	0.667 59	0.0366	2.970	- 0.131	
2.033	0.669 79	0.0439	2.950	- 0.141	
2.633	0.705 43	0.0669	2.760	- 0.291	
3.233	0.750 11	0.0730	2.550	- 0.359	
3.833	0.793 08	0.0682	2.420	- 0.410	
4.433	0.831 90	0.0590	2.300	- 0.449	
5.033	0.863 88	0.0476	2.200	- 0.480	
5.633	0.889 03	0.0321	2.130	- 0.500	

Note: the last decimal places in this Table are not significant

Table 2/

Table 2

Crocco-Lees parameters for zero suction, but with a cooled wall, with $H_w = 0.6$

ψ	K	K'	C	σ	Remarks
0.720	0.703 92	- 0.1196	2.239	1.289	
0.770	0.698 06	- 0.1196	2.419	1.000	Constant pressure
0.820	0.691 96	- 0.1099	2.534	0.793	
0.870	0.687 08	- 0.1099	2.650	0.641	
0.920	0.680 97	- 0.1099	2.755	0.520	
0.970	0.676 09	- 0.1001	2.847	0.420	
1.020	0.670 96	- 0.0903	2.919	0.340	
1.070	0.667 06	- 0.0708	2.974	0.275	
1.120	0.663 88	- 0.0610	3.021	0.221	
1.170	0.660 95	- 0.0391	3.069	0.168	
1.220	0.659 98	- 0.0195	3.110	0.119	
1.270	0.659 00	- 0.0098	3.140	0.076	
1.320	0.659 00	+ 0.0098	3.159	0.035	
1.370	0.659 98	0.0195	3.169	0	Separation
1.420	0.660 95	0.0195	3.150	- 0.027	
1.470	0.661 93	0.0201	3.130	- 0.051	
1.670	0.668 03	0.0427	3.021	- 0.119	
1.870	0.679 02	0.0598	2.919	- 0.178	
2.070	0.691 96	0.0775	2.819	- 0.225	
2.270	0.710 03	0.0928	2.720	- 0.260	
2.470	0.729 07	0.0977	2.620	- 0.289	
2.670	0.749 09	0.1025	2.523	- 0.316	
2.870	0.770 08	0.1025	2.431	- 0.340	
3.070	0.790 10	0.0995	2.341	- 0.361	
3.270	0.809 88	0.0995	2.249	- 0.381	

Note: the last decimal places in this Table are not significant.

Table 3/

Table 3

Crocco-Lees parameters for zero heat transfer or suction, with velocity ratio at edge taken as 0.98

ψ	K	K'	C	σ	Remarks
0.820	0.768 77	- 0.1611	3.750	1.181	Constant pressure
0.870	0.760 96	- 0.1440	4.051	0.880	at ψ = 0.850
0.920	0.754 37	- 0.1245	4.221	0.681	
0.970	0.748 51	- 0.1099	4.350	0.540	
1.020	0.743 38	- 0.0952	4.430	0.431	
1.070	0.738 98	- 0.0806	4.500	0.329	
1.120	0.735 32	- 0.0659	4.541	0.249	
1.170	0.732 39	- 0.0464	4.590	0.190	
1.220	0.730 68	- 0.0269	4.619	0.130	
1.270	0.729 71	- 0.0146	4.631	0.079	
1.320	0.729 22	- 0.0073	4.641	0.040	
1.370	0.728 97	0	4.650	- 0.001	Separation
1.420	0.729 22	+ 0.0098	4.641	- 0.040	
1.470	0.729 95	0.0220	4.631	- 0.069	
1.520	0.731 42	0.0317	4.619	- 0.101	
1.570	0.733 13	0.0391	4.609	- 0.120	
1.620	0.735 32	0.0488	4.600	- 0.149	
1.670	0.738 01	0.0537	4.580	- 0.171	
1.720	0.740 69	0.0586	4.560	- 0.190	
1.770	0.743 87	0.0684	4.541	- 0.200	
1.820	0.747 53	0.0681	4.519	- 0.220	
2.270	0.785 62	0.0740	4.301	- 0.329	
2.720	0.821 50	0.0674	4.100	- 0.399	
3.170	0.853 00	0.0576	3.930	- 0.460	
3.620	0.879 12	0.0488	3.779	- 0.489	
4.070	0.901 83	0.0435	3.660	- 0.520	
4.520	0.922 58	0.0413	3.580	- 0.540	

Note: the last decimal places in this Table are not significant.

Table 4/

Table 4

Crocco-Lees parameters for zero heat transfer, but with suction, with G = 0.4

Basic solutions computed by A. R. Curtis: values in brackets obtained by interpolation

ψ	K	$(1 - K)\sigma$	F_e^{-1}	β	Remarks
0.9206	0.7337	0.5796	0.7464	0	Constant pressure
0.9353	0.7313	0.5383	0.7341	- 0.04	
0.9523	0.7286	0.4959	0.7216	- 0.08	
0.9723	0.7256	0.4520	0.7089	- 0.12	
0.9962	0.7222	0.4062	0.6960	- 0.16	
1.0255	0.7182	0.3580	0.6829	- 0.20	
1.0626	0.7136	0.3061	0.6696	- 0.24	
1.1122	0.7080	0.2486	0.6559	- 0.28	
1.1860	0.7011	0.1806	0.6418	- 0.32	
1.3346	0.6919	0.0818	0.6271	- 0.36	
1.4379	0.6888	0.03152	0.6232	- 0.37	
(1.5160)	(0.6880)	0	(0.6224)	(- 0.3719)	Separation
1.6046	0.6889	- 0.03024	0.6232	- 0.37	
1.7611	0.6940	- 0.0736	0.6276	- 0.36	
2.1415	0.7209	- 0.1428	0.6471	- 0.32	
2.4830	0.7568	- 0.1785	0.6693	- 0.28	
2.8488	0.8018	- 0.2005	0.6944	- 0.24	
3.2697	0.8570	- 0.2129	0.7229	- 0.20	
3.7835	0.9243	- 0.2168	0.7555	- 0.16	
4.4543	1.0068	- 0.2112	0.7936	- 0.12	
5.4265	1.1098	- 0.1933	0.8392	- 0.08	
7.1717	1.2437	- 0.1541	0.8967	- 0.04	

Table 5/

Table 5

Cases calculated by the Crocco-Lees method

Case No.	M_o	H_w	C	ζ_s	10^{-5} R_{xs}	Remarks
1	2	1	0	445.3	1.26	$w_\infty = 1.3615$. Repeat of Bray's calculations using original type of parameters (not lower branch)
2	2	1	0	445.3	1.26	As 1, but lower-branch functions used (Table 1)
3	3	1	0	560	4.87	Find w_∞ just to separate (Table 1)
4	3	1	0	560	4.87	$w_\infty = 1.71$ (Table 1)
5	3	1	0	714	4.92	$w_\infty = 1.71$ (Table 3)
6	3	1	0	560	-	Find w_∞ just to separate: parameters as in Table 1 but with C doubled
7	3	0.6	0	560	4.90	Find w_∞ just to separate (Table 2)
8	3	0.6	0	560	4.90	$w_\infty = 1.71$ (Table 2)
9	3	1	0.4	480	4.90	Find w_∞ just to separate (Table 4)
10	3	1	0.4	480	4.90	$w_\infty = 1.71$ (Table 4)
11	3	1	0	250	0.94	Find w_∞ just to separate (Table 1)
12	3	1	0	250	0.94	$w_\infty = 1.71$ (Table 1)
13	3	1	0	250	0.94	Extension of laminar foot of cases 11 and 12 (Table 1)
14	3	0.6	0	250	0.95	Find laminar foot (Table 2)
15	3	0.6	0	560	4.90	Extension of laminar foot of cases 7 and 8 (Table 2)
16	3	1	0	1250	24.8	Find laminar foot (Table 1)
17	3	0.6	0	1250	24.8	Find laminar foot (Table 2)
18	1.4	1	0	1130	4.97	Find w_∞ just to separate (Table 1)
19	1.4	1	0.4	970	4.97	Find w_∞ just to separate (Table 4)

Table 6/

Table 6

Parameters for method of Section 8, from the similarity solutions for zero heat transfer or suction

r	$\left(\frac{\partial f}{\partial \ell}\right)_w$	$\left(\frac{\partial^2 f}{\partial \ell^2}\right)_w$	Remarks
2.16	0.389	- 0.1063	
2.17	0.381	- 0.1000	
2.22	0.360	- 0.0855	
2.30	0.325	- 0.0611	
2.41	0.280	- 0.0333	
2.59	0.221	0	Constant pressure (with no suction)
2.80	0.164	+ 0.0266	
3.09	0.105	0.0488	
4.03	0	0.0682	Separation
5.52	- 0.0540	0.0559	
7.42	- 0.0663	0.0378	
12.63	- 0.0546	0.0150	
28.1	- 0.0257	0.0028	
59.3	- 0.0107	0.0005	

Table 7

Parameters for method of Section 8, for zero suction, but with a cooled wall, with $H_w = 0.6$

$$\left(\frac{\partial f}{\partial \ell}\right)_{wc} = 0.221$$

r_1	$\left(\frac{\partial^2 f}{\partial \ell^2}\right)_w$	Remarks
0.759	- 0.1040	
1.185	- 0.0433	
1.556	0	Constant pressure
2.034	0.0369	
2.399	0.0495	
2.679	0.0537	
3.063, 3.041*	0.0531, 0.0540*	Separation
3.623	0.0491	
6	0.0309†	
8	0.0210†	
10	0.0146†	

*There appear to be slight inconsistencies in Cohen and Reshotko's data, and alternative methods of estimation give alternative answers.

†Obtained by extrapolation.

Table 8/

Table 8

$Q^{\frac{1}{2}}$ and $\int_{r_s}^{r} \frac{dr}{Q^{\frac{1}{2}}}$ for cases with zero suction. method A

$r-r_c$	$Q^{\frac{1}{2}}$	$\int_{r_s}^{r} \frac{dr}{Q^{\frac{1}{2}}}$	$r-r_c$	$Q^{\frac{1}{2}}$	$\int_{r_s}^{r} \frac{dr}{Q^{\frac{1}{2}}}$
0.2	0.0529	- 8.59	13.0	0.6460	22.35
0.6	0.1400	- 4.16	13.4	0.6490	22.96
1.0	0.2083	- 1.85	13.8	0.6521	23.58
1.4	0.2648	- 0.16	14.2	0.6550	24.19
1.8	0.3119	+ 1.23	14.6	0.6577	24.80
2.2	0.3517	2.43	15.0	0.6600	25.41
2.6	0.3852	3.52	15.4	0.6625	26.01
3.0	0.4134	4.52	15.8	0.6648	26.61
3.4	0.4377	5.46	16.2	0.6672	27.21
3.8	0.4588	6.35	16.6	0.6693	27.81
4.2	0.4775	7.21	17.0	0.6712	28.41
4.6	0.4950	8.03	17.4	0.6732	29.01
5.0	0.5091	8.83	17.8	0.6749	29.60
5.4	0.5226	9.60	18.2	0.6767	30.19
5.8	0.5350	10.36	18.6	0.6784	30.78
6.2	0.5462	11.10	19.0	0.6801	31.35
6.6	0.5563	11.82	19.4	0.6816	31.96
7.0	0.5655	12.54	19.8	0.6830	32.54
7.4	0.5741	13.24	20.2	0.6843	33.13
7.8	0.5819	13.93	20.6	0.6855	33.71
8.2	0.5892	14.61	21.0	0.6867	34.30
8.6	0.5929	15.29	21.4	0.6878	34.88
9.0	0.6021	15.96	21.8	0.6890	35.46
9.4	0.6080	16.62	22.2	0.6900	36.04
9.8	0.6133	17.27	22.6	0.6913	36.62
10.2	0.6183	17.92	23.0	0.6923	37.20
10.6	0.6229	18.57	23.4	0.6934	37.77
11.0	0.6274	19.21	23.8	0.6944	38.35
11.4	0.6316	19.84	24.2	0.6954	38.93
11.8	0.6354	20.47	24.6	0.6962	39.50
12.2	0.6392	21.10	25.0	0.6970	40.07
12.6	0.6429	21.72			

Table 9/

Table 9

$Q^{\frac{1}{2}}$ and $\int_{r_s}^{r} \frac{dr}{T Q^{\frac{1}{2}}}$ for cases with cooled wall, method B

$r-r_c$	$Q^{\frac{1}{2}}$	$\int_{r_s}^{r} \frac{dr}{T Q^{\frac{1}{2}}}$
0.2	0.0474	- 9.75
0.6	0.1255	- 4.83
1.0	0.1873	- 2.25
1.4	0.2378	- 0.37
1.8	0.2789	+ 1.18
2.2	0.3126	2.53
2.6	0.3407	3.76
3.0	0.3648	4.89
3.4	0.3858	5.95
3.8	0.4041	6.97
4.2	0.4205	7.94
4.6	0.4350	8.86
5.0	0.4482	9.78
5.4	0.4599	10.66
5.8	0.4706	11.52
6.2	0.4802	12.36
6.6	0.4890	13.18
7.0	0.4970	14.00
7.4	0.5042	14.79
7.8	0.5109	15.58
8.2	0.5170	16.36
8.6	0.5226	17.13
9.0	0.5280	17.89

Table 10/

Table 10

$Q^{\frac{1}{2}}$ and $\int_{r_s}^{r} \frac{dr}{Q^{\frac{1}{2}}}$ for cases with suction, method A

$r-r_c$	$Q^{\frac{1}{2}}$	$\int_{r_s}^{r} \frac{dr}{Q^{\frac{1}{2}}}$	$r-r_c$	$Q^{\frac{1}{2}}$	$\int_{r_s}^{r} \frac{dr}{Q^{\frac{1}{2}}}$
0.2	0.0730	- 7.78	13.0	0.5895	22.56
0.6	0.1697	- 4.40	13.4	0.5899	22.57
1.0	0.2358	- 2.43	13.8	0.5901	23.25
1.4	0.2886	- 0.90	14.2	0.5902	23.93
1.8	0.3332	+ 0.39	14.6	0.5903	24.60
2.2	0.3711	1.52	15.0	0.5902	25.28
2.6	0.4032	2.55	15.4	0.5901	25.96
3.0	0.4293	3.51	15.8	0.5899	26.64
3.4	0.4510	4.42	16.2	0.5895	27.22
3.8	0.4693	5.29	16.6	0.5891	27.99
4.2	0.4850	6.11	17.0	0.5884	28.67
4.6	0.4985	6.94	17.4	0.5877	29.35
5.0	0.5104	8.19	17.8	0.5870	30.03
5.4	0.5207	8.48	18.2	0.5865	30.62
5.8	0.5295	9.25	18.6	0.5856	31.40
6.2	0.5372	10.00	19.0	0.5848	32.08
6.6	0.5441	10.74	19.4	0.5837	32.77
7.0	0.5501	11.47	19.8	0.5825	33.45
7.4	0.5554	12.19	20.2	0.5816	34.14
7.8	0.5605	12.91	20.6	0.5805	34.83
8.2	0.5647	13.62	21.0	0.5796	35.52
8.6	0.5686	14.33	21.4	0.5784	36.21
9.0	0.5721	15.03	21.8	0.5774	36.90
9.4	0.5753	15.73	22.2	0.5761	37.59
9.8	0.5779	16.42	22.6	0.5748	38.29
10.2	0.5803	17.11	23.0	0.5734	38.99
10.6	0.5822	17.80	23.4	0.5721	39.68
11.0	0.5840	18.49	23.8	0.5708	40.38
11.4	0.5855	19.17	24.2	0.5695	41.08
11.8	0.5868	19.85	24.6	0.5681	41.78
12.2	0.5881	20.53	25.0	0.5669	41.82
12.6	0.5888	21.21			

WS

FIGS. 1 & 2.

FIG. 1.

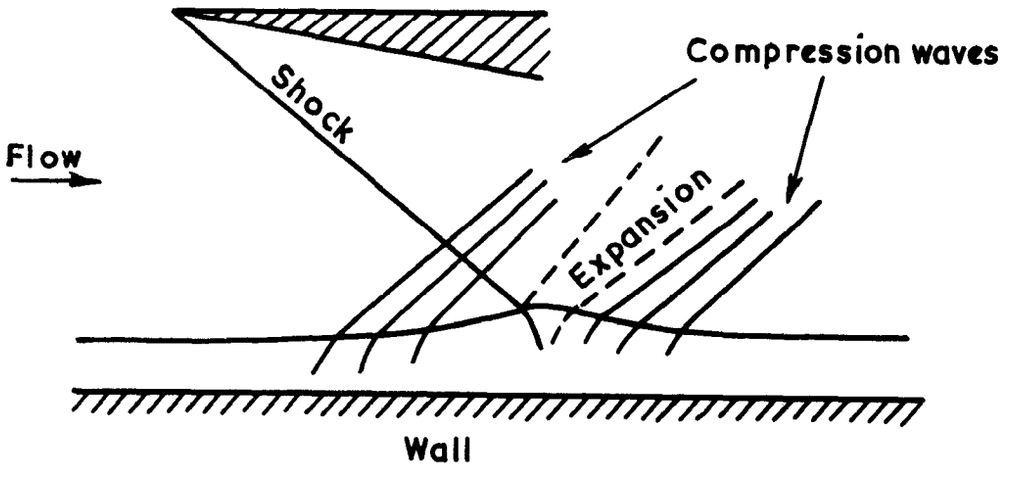

Interaction between an oblique shock and a boundary layer

FIG. 2.

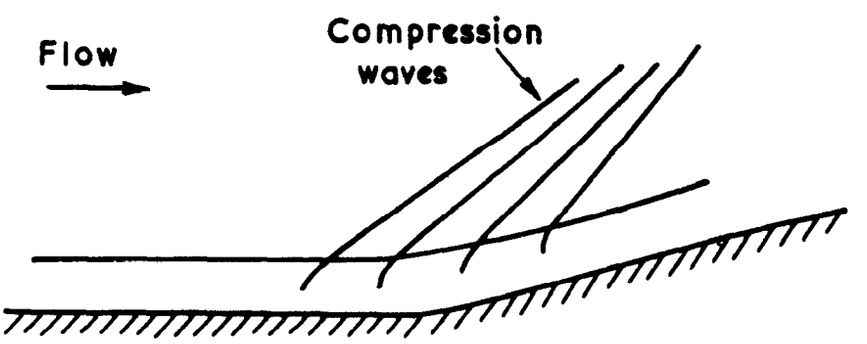

Wall with an abrupt change of slope

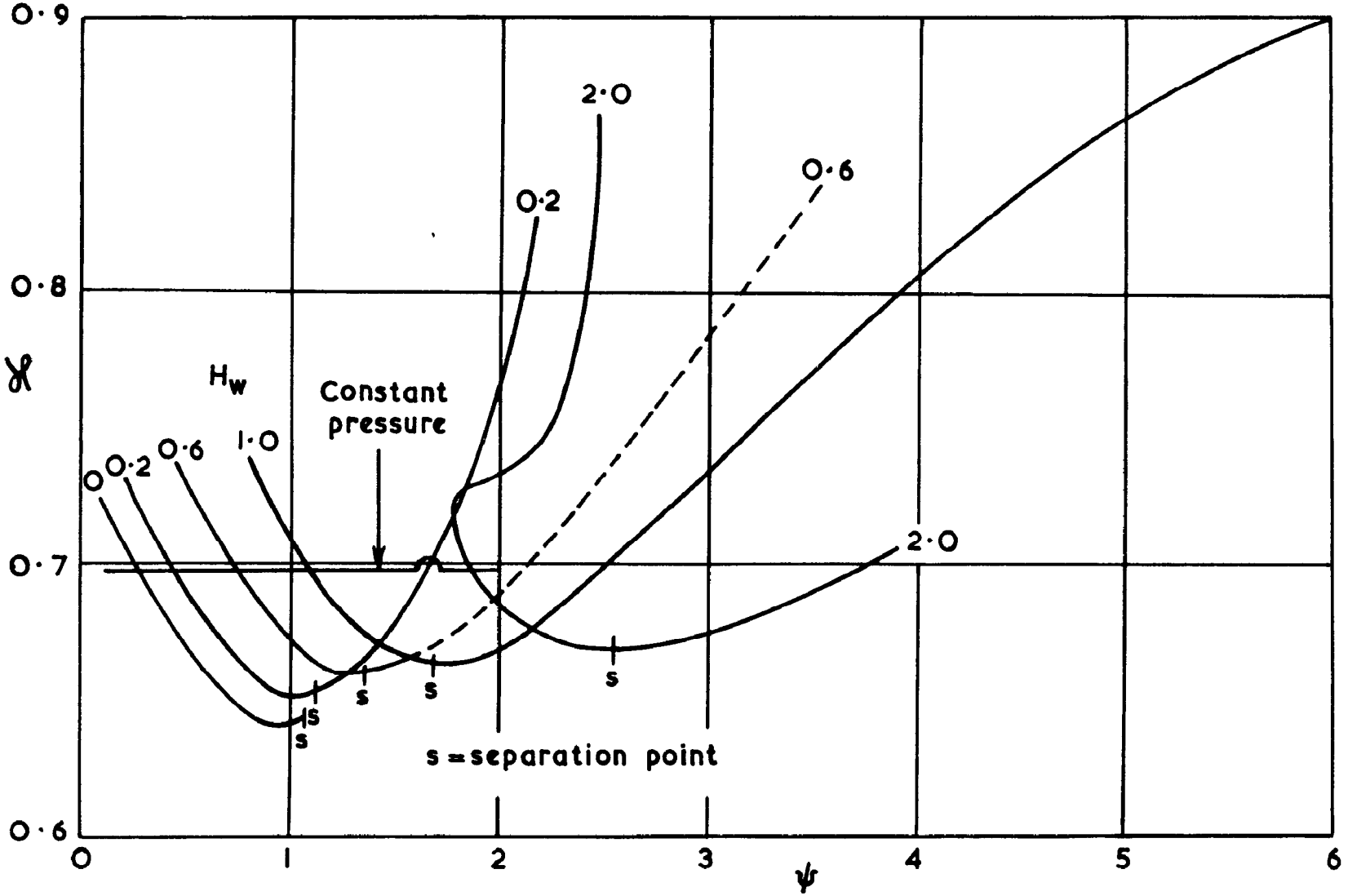

χ as a function of ψ for various wall temperature ratios

FIG. 3.

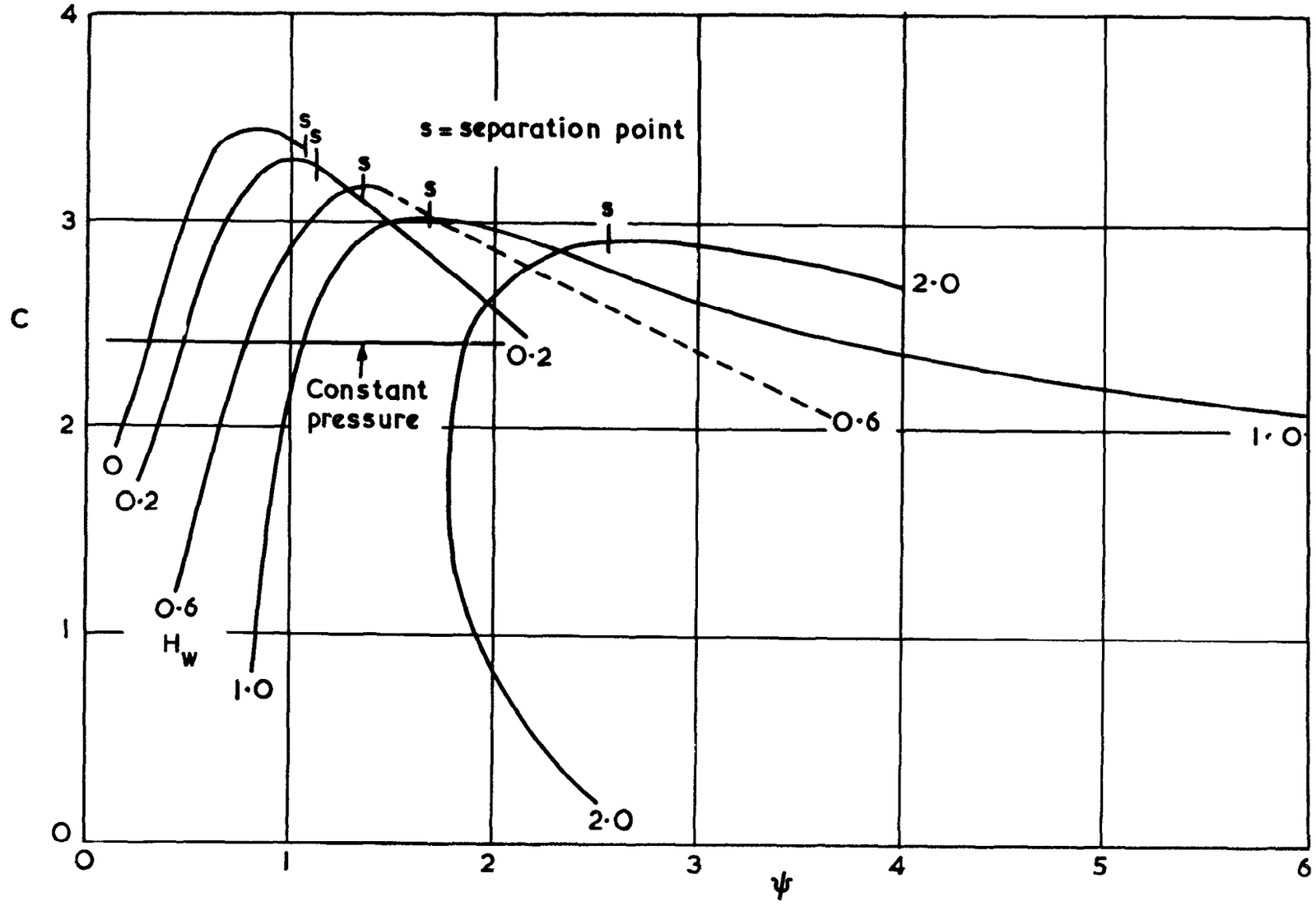

C as a function of ψ for various wall temperature ratios.

FIG. 4.

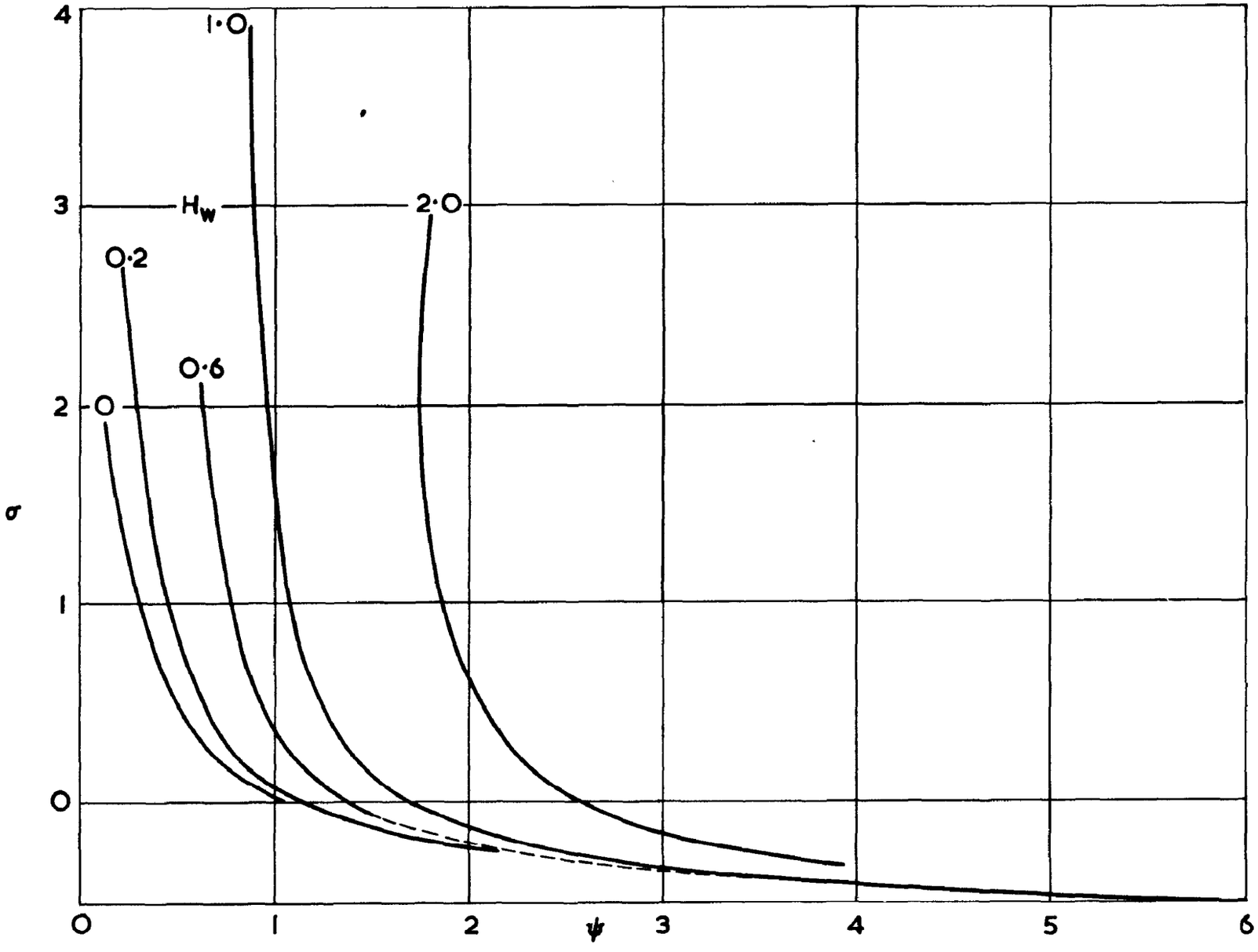

σ as a function of ψ for various wall temperature ratios.

FIG. 5.

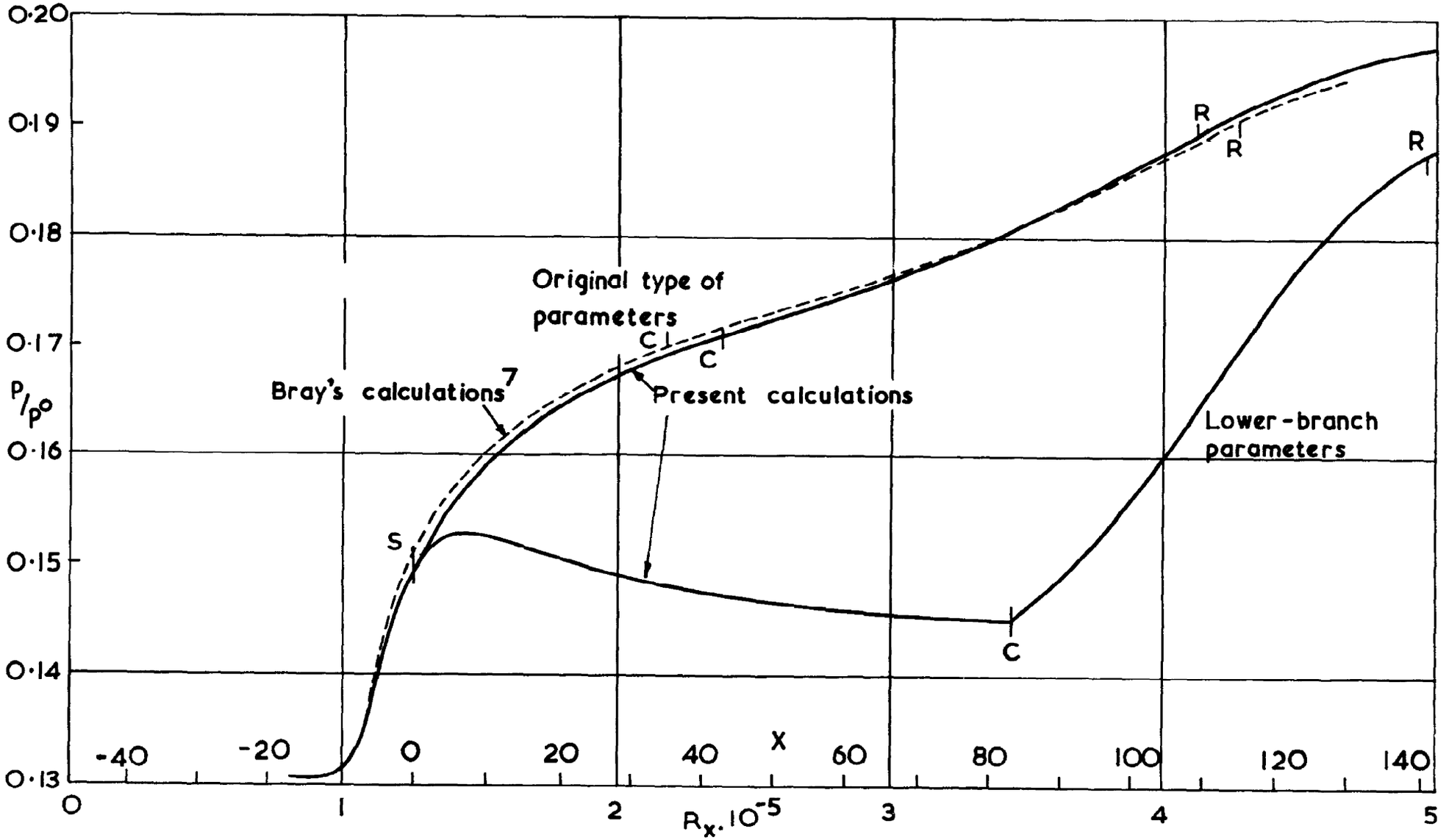

FIG. 6.

Pressure distributions for a case computed by Bray, at $M_0 = 2$.

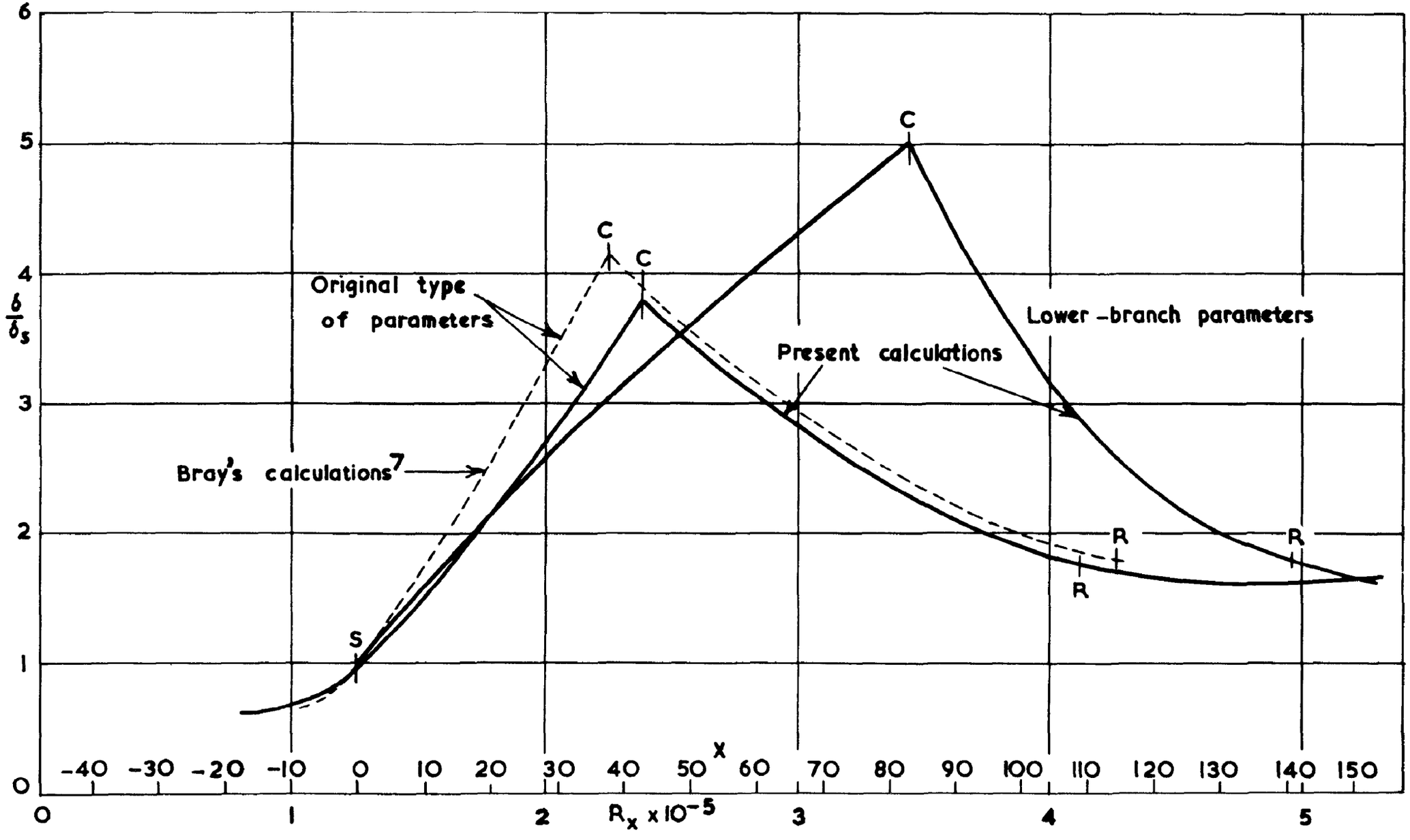

FIG. 7.

Variation of boundary-layer thickness for a case computed by Bray at $M_0 = 2$

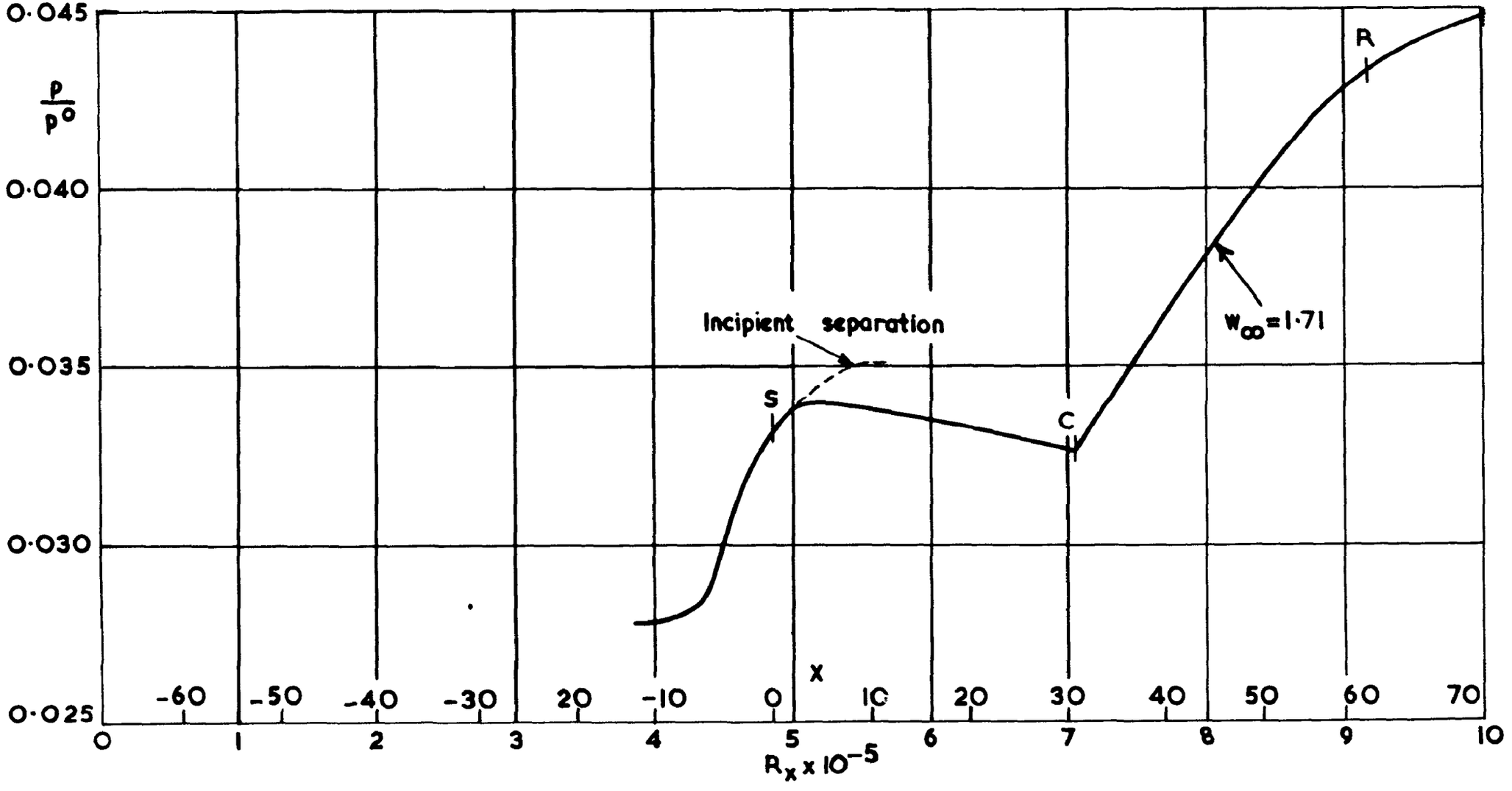

FIG. 8.

Pressure distributions with incipient and extensive separation at $M_0 = 3$

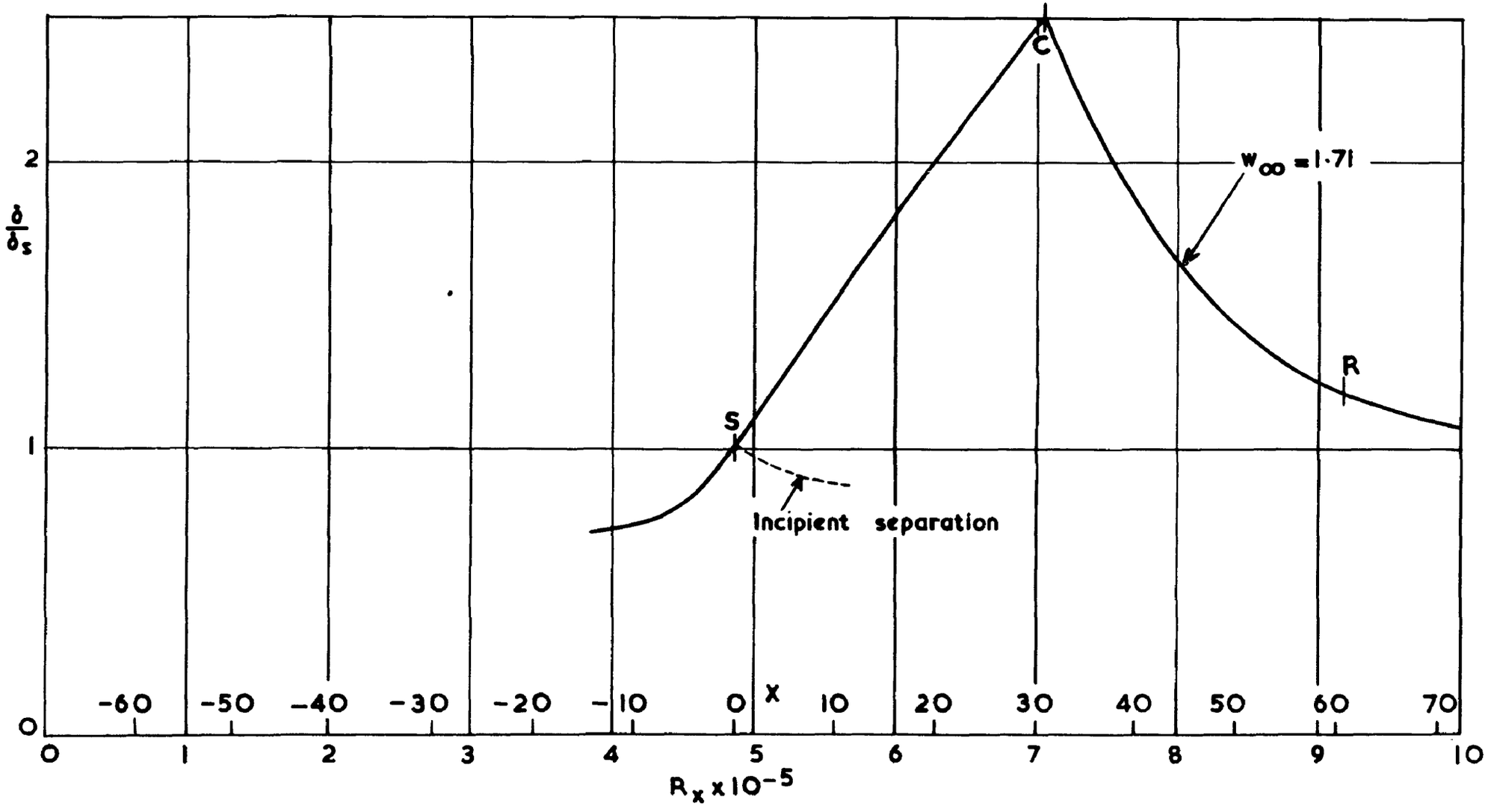

FIG.9.

Boundary-layer thickness distributions with incipient and extensive separation at $M_0 = 3$.

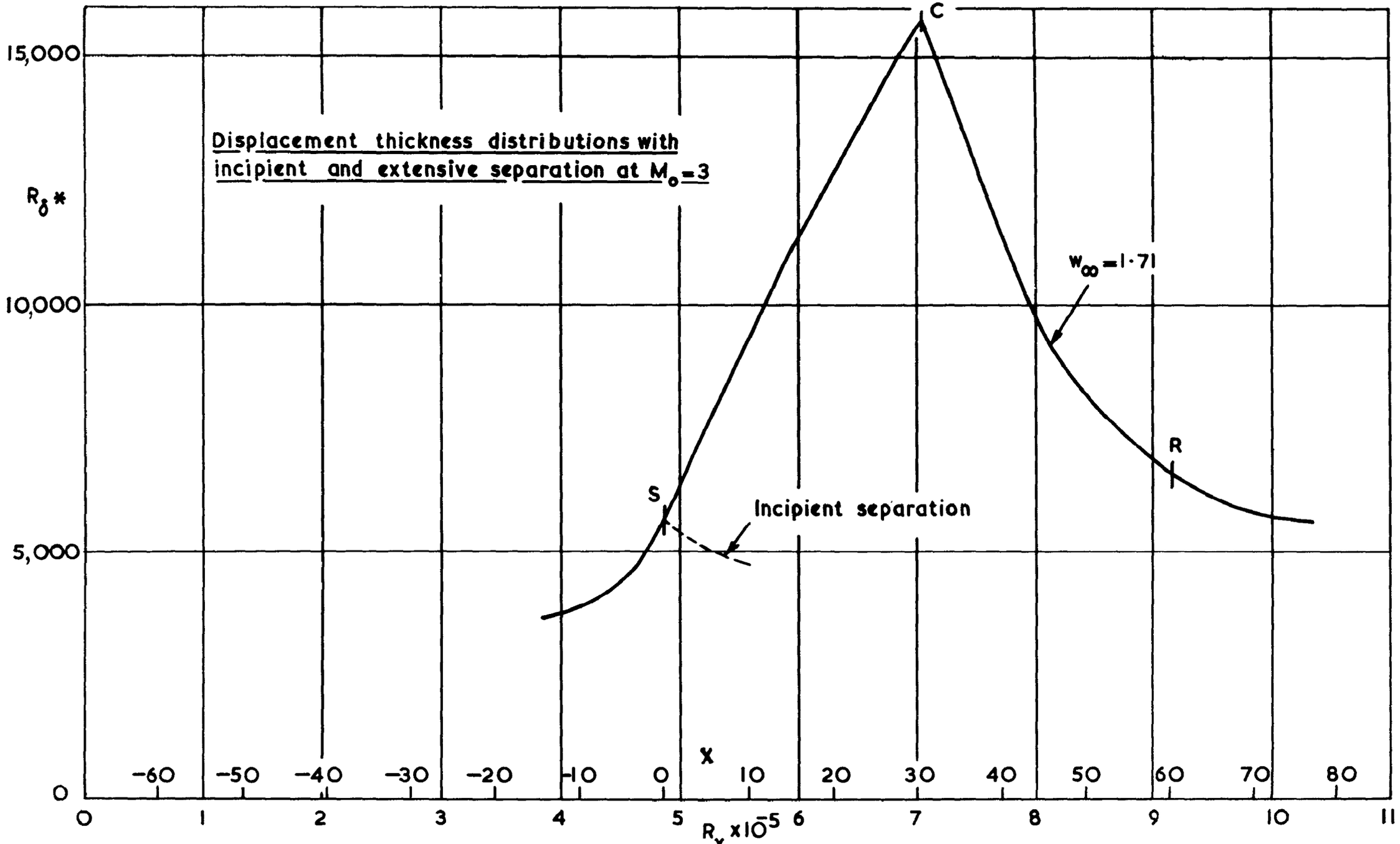
Displacement thickness distributions with incipient and extensive separation at $M_0=3$
R_δ^*
15,000
10,000
5,000
0
C
$w_\infty=1\cdot71$
R
S
Incipient separation
X
−60 −50 −40 −30 −20 −10 0 10 20 30 40 50 60 70 80
0 1 2 3 4 5 6 7 8 9 10 11
$R_x \times 10^{-5}$

FIG. 10.

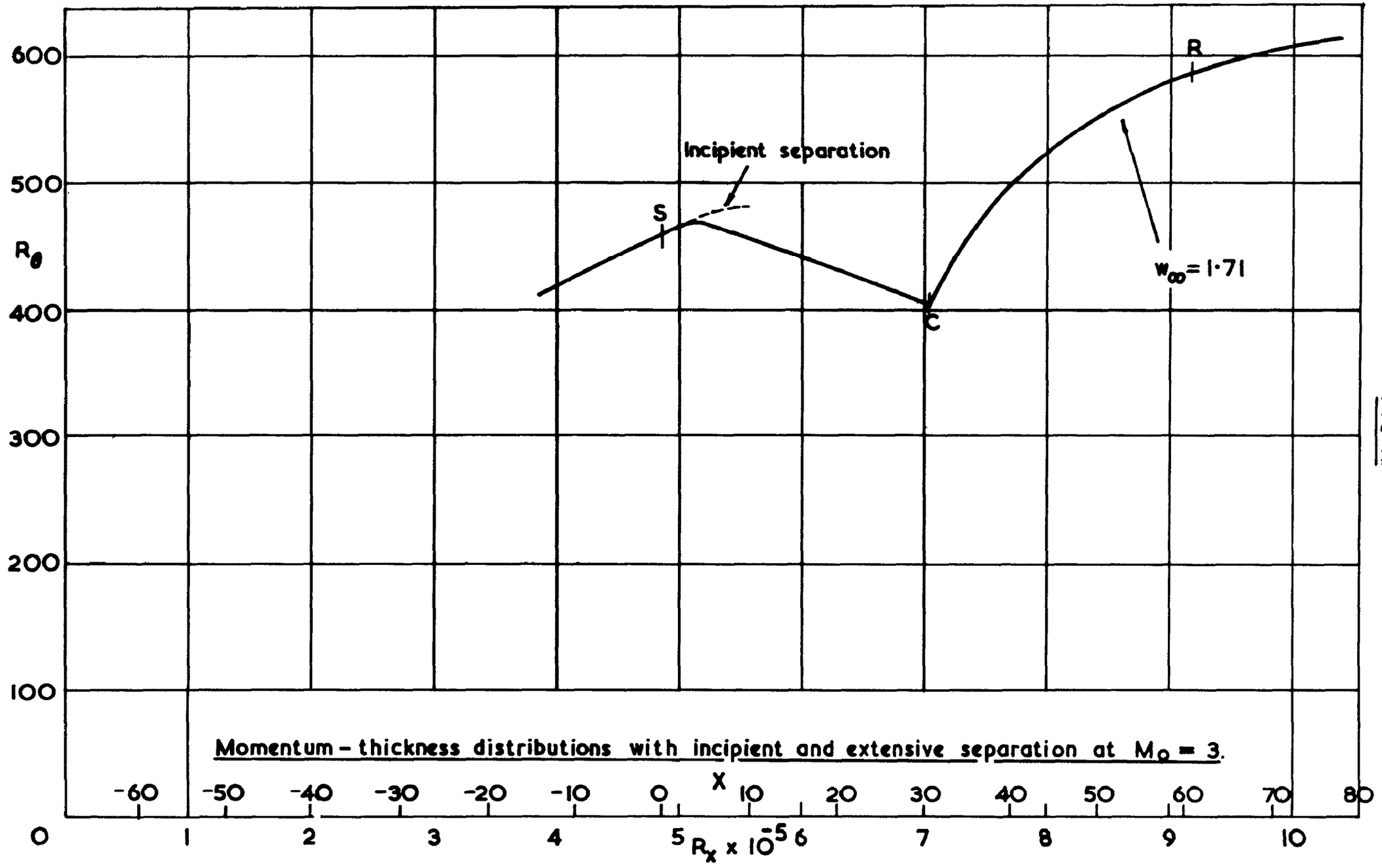

Momentum – thickness distributions with incipient and extensive separation at $M_0 = 3$.

FIG. 11.

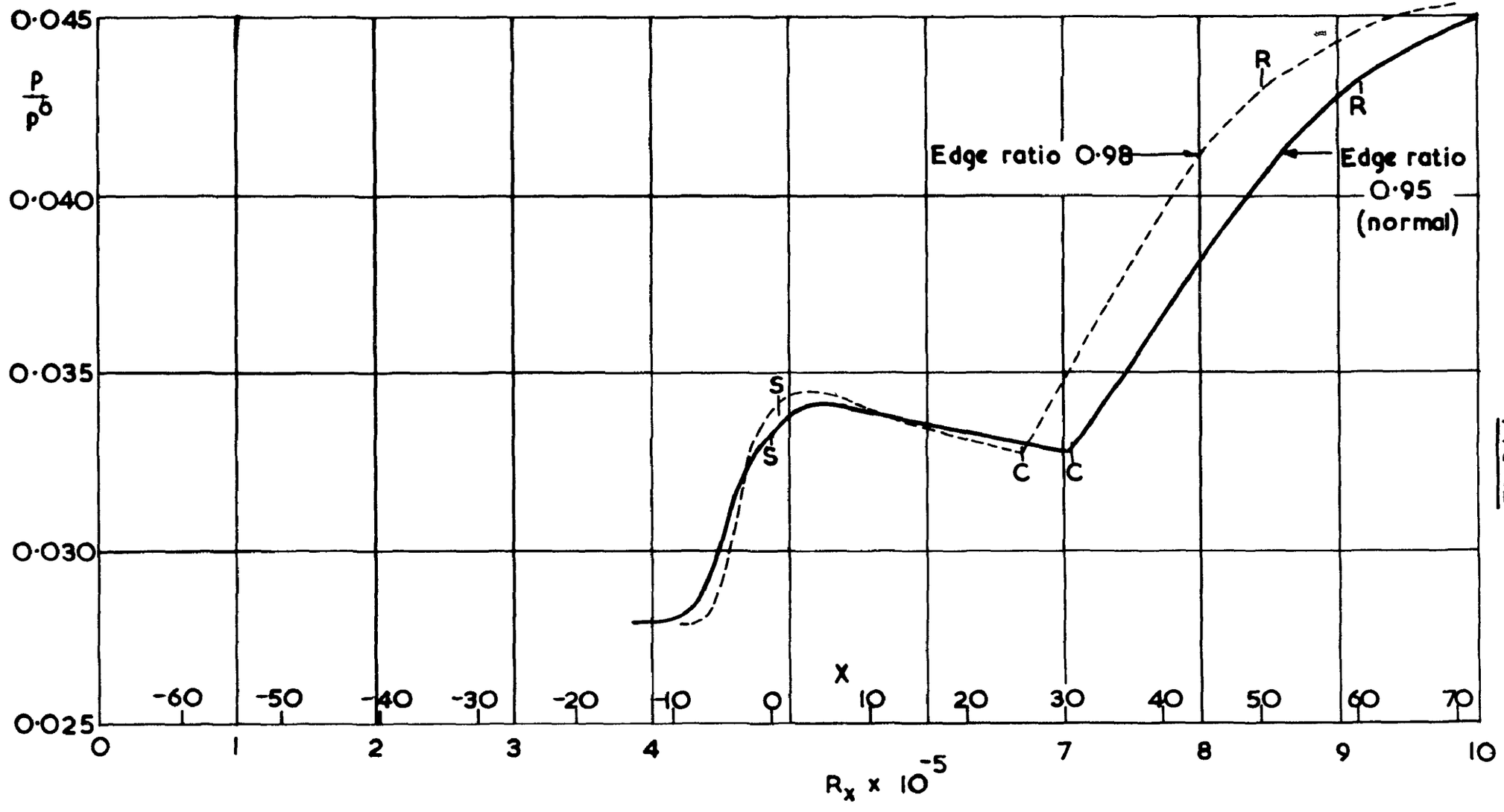

FIG.12.

The effect of varying the definition of the edge of the layer for calculations of a case with extensive separation at $M_0 = 3$.

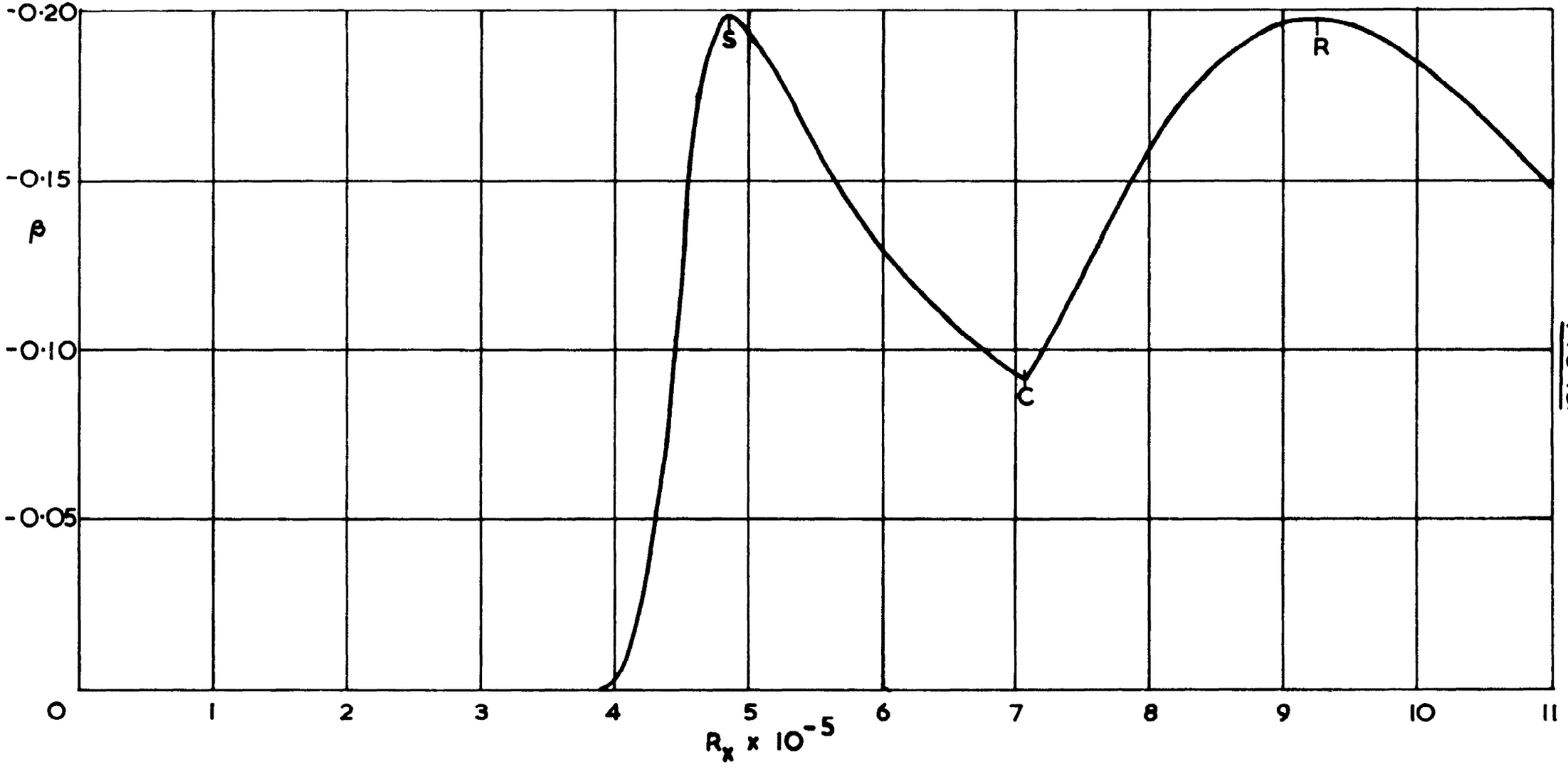

FIG 13.

Distribution of equivalent β for a case with extensive separation at $M_0 = 3$.

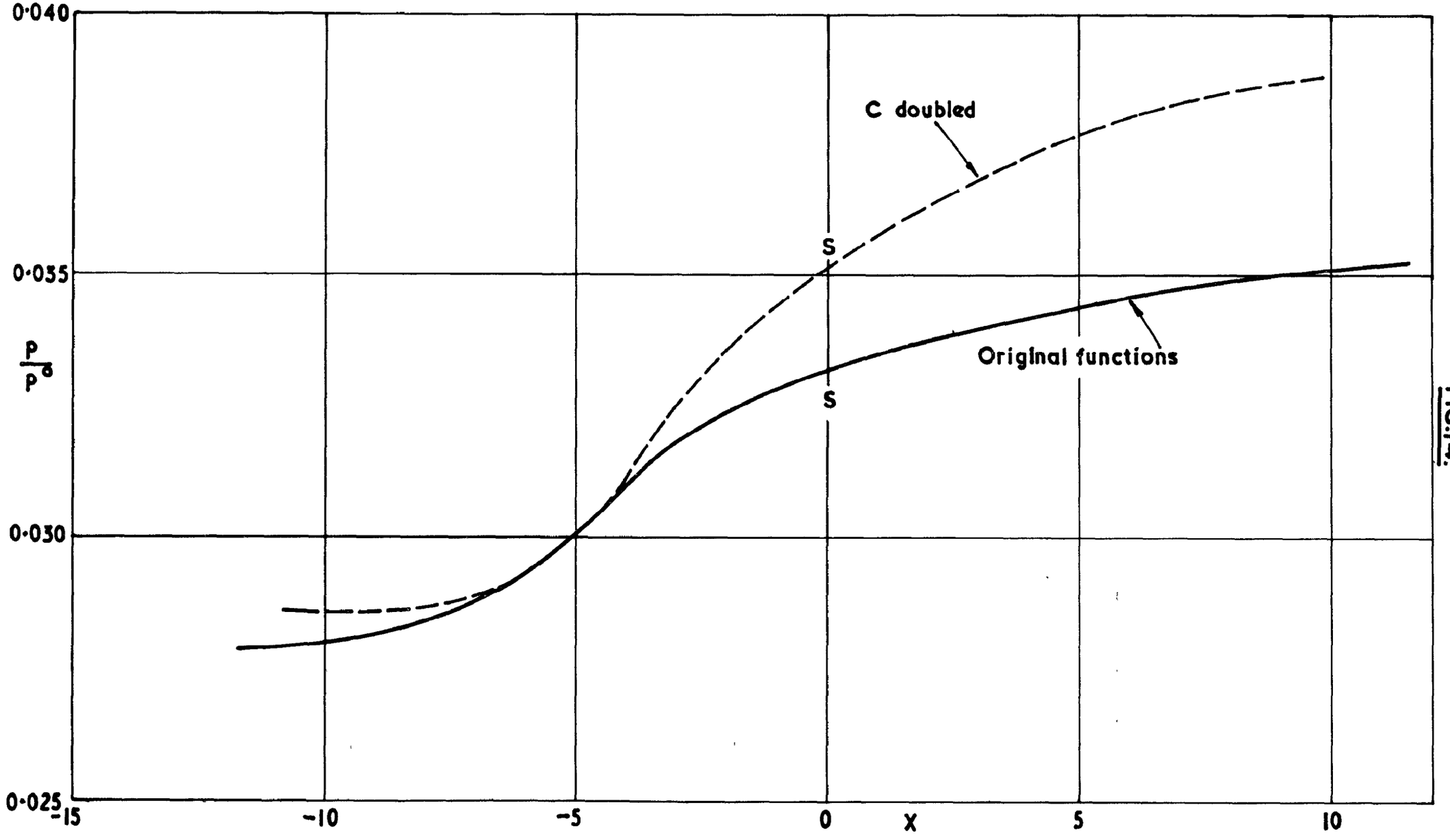

FIG.14.

The effect of doubling C on the pressure distribution for a case with incipient separation at $M_0 = 3$

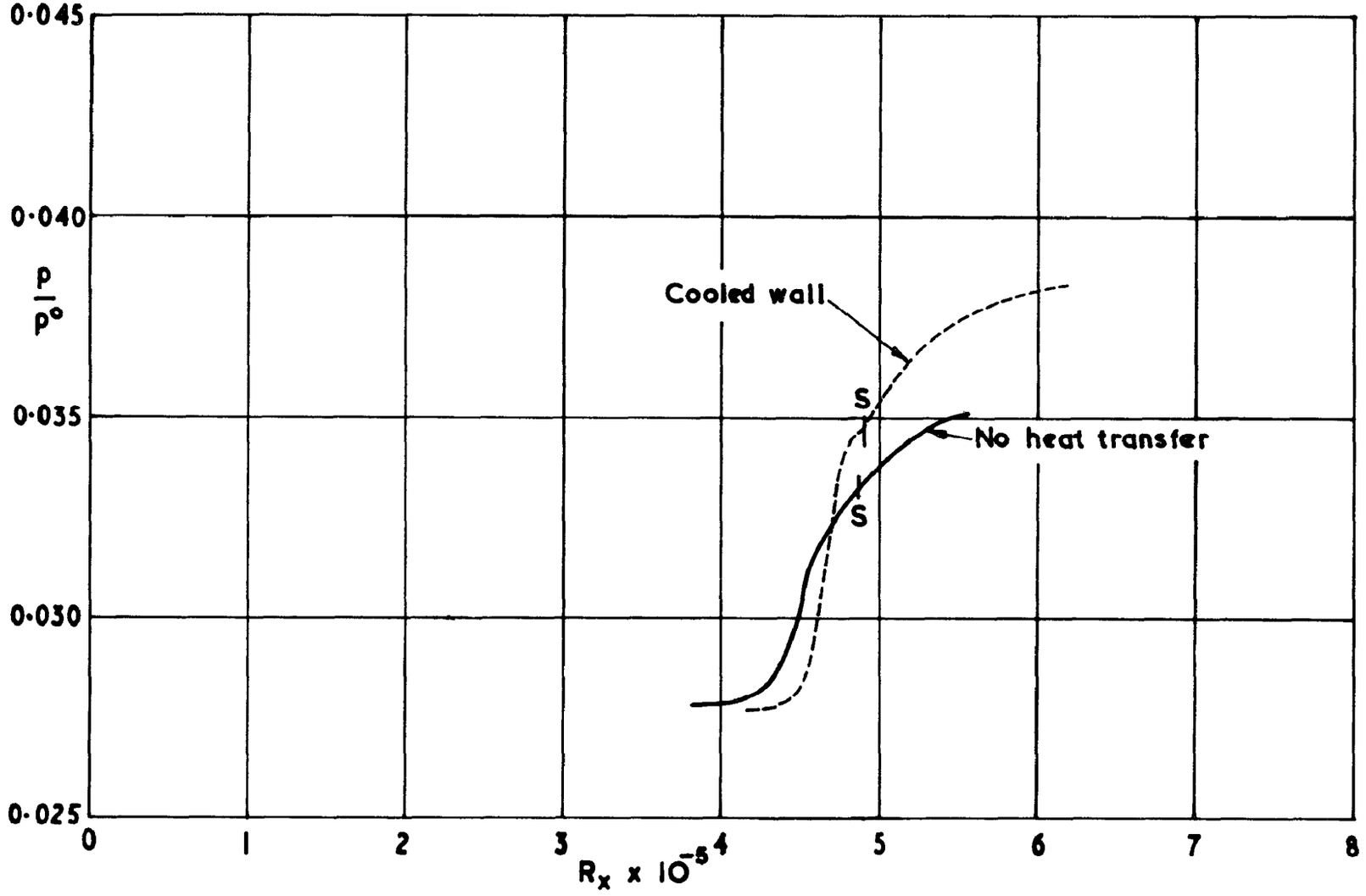

FIG. 15.

Calculated effects of cooling the wall on a case with incipient separation at $M_o = 3$

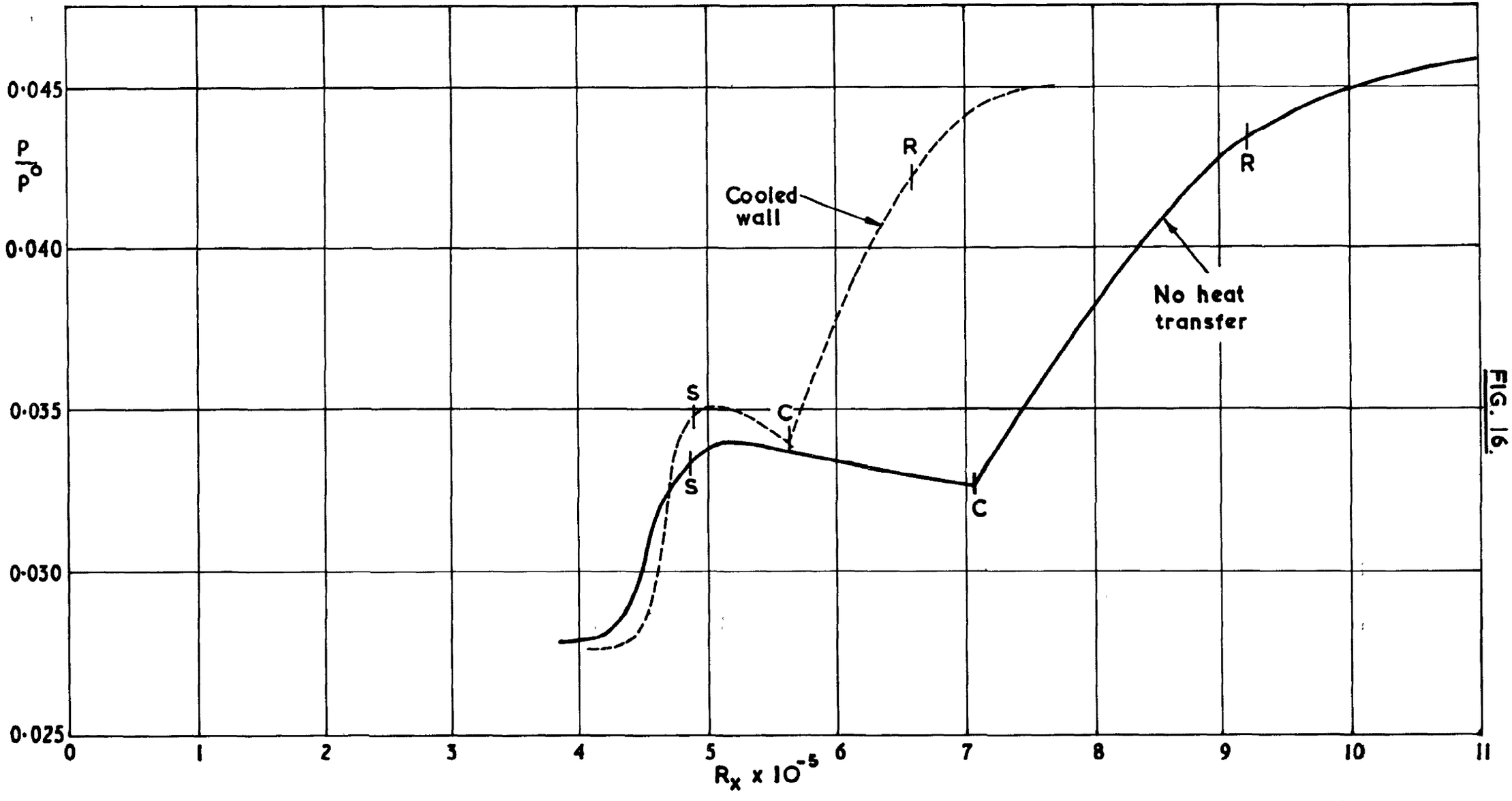

FIG. 16.

Calculated effects of cooling the wall on a case with extensive separation at $M_o = 3$.

FIG. 17

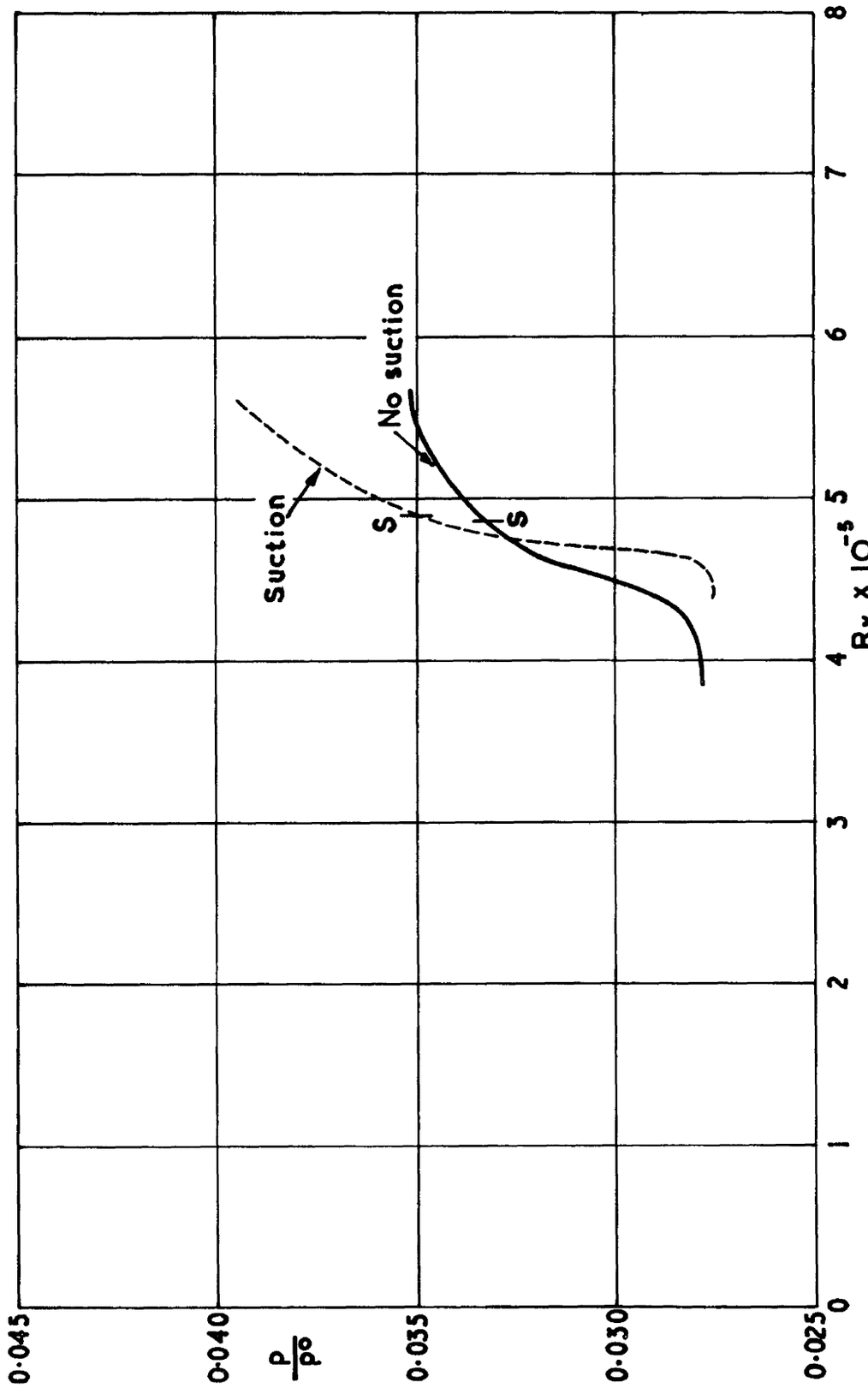

Calculated effects of suction on a case with incipient separation at $M_o = 3$

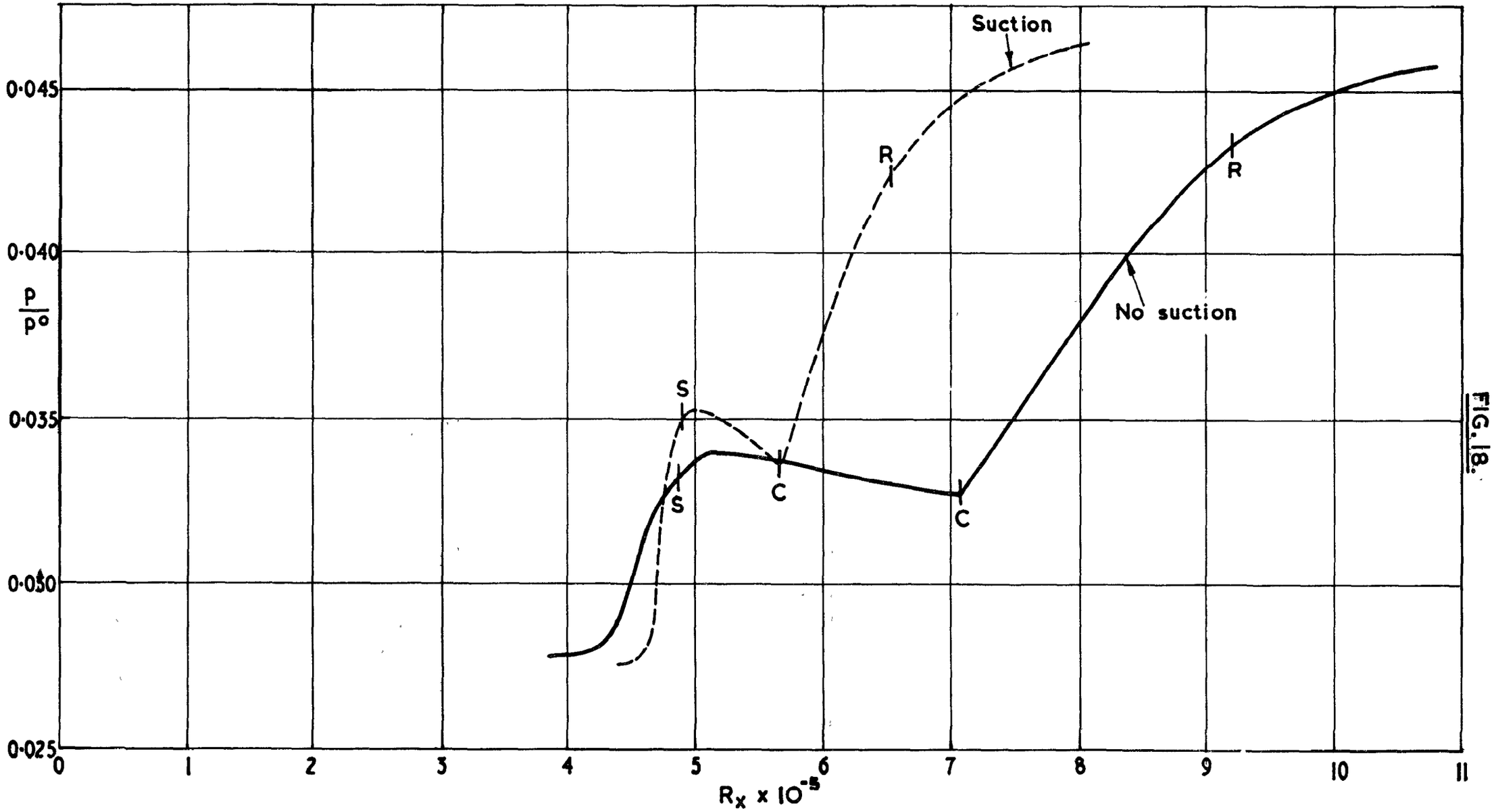

FIG. 18.

Calculated effects of suction on a case with extensive separation at $M_o = 3$

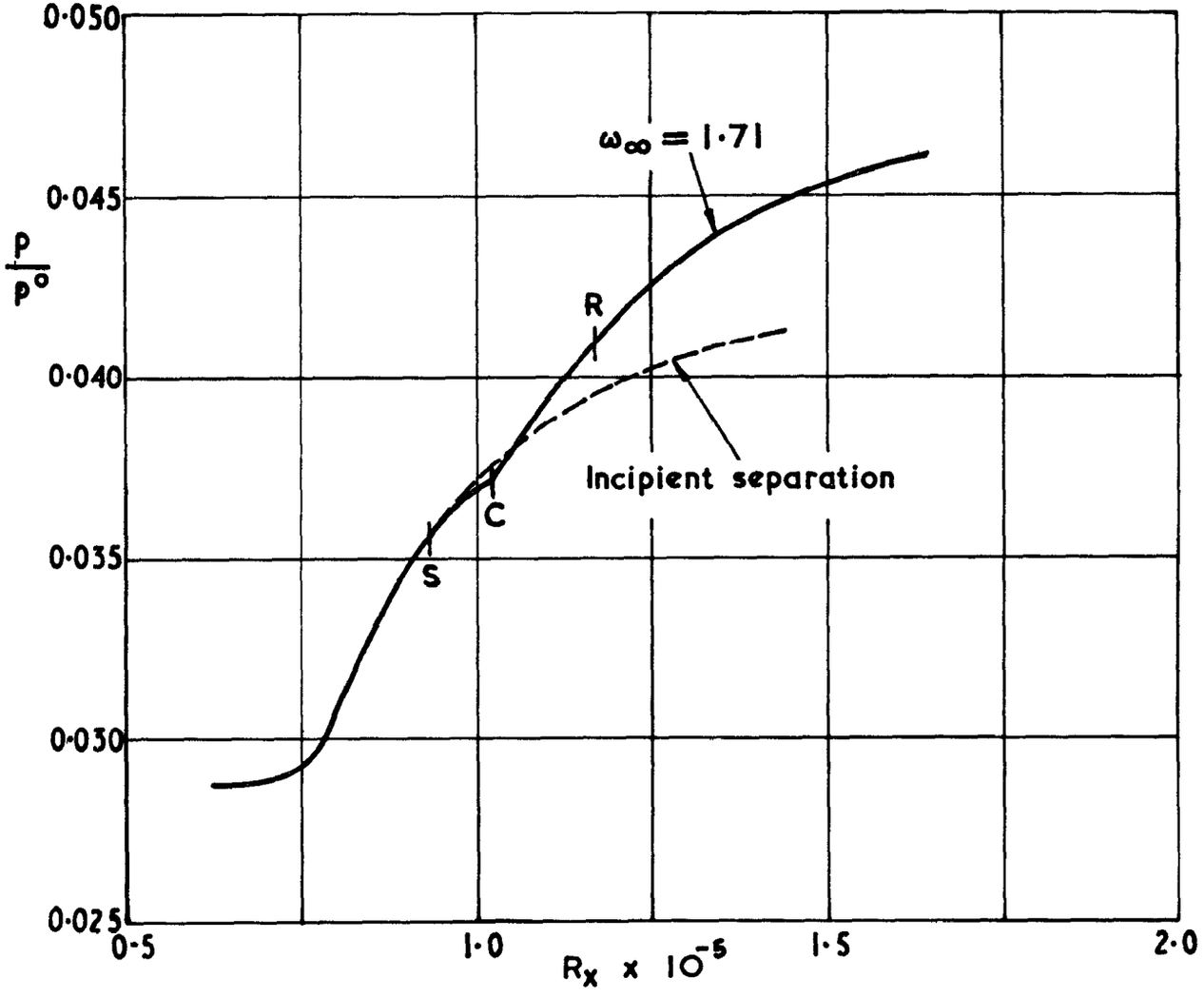

FIG. 19

Pressure distributions with incipient and moderate separation at $M_0 = 3$ and a low Reynolds number

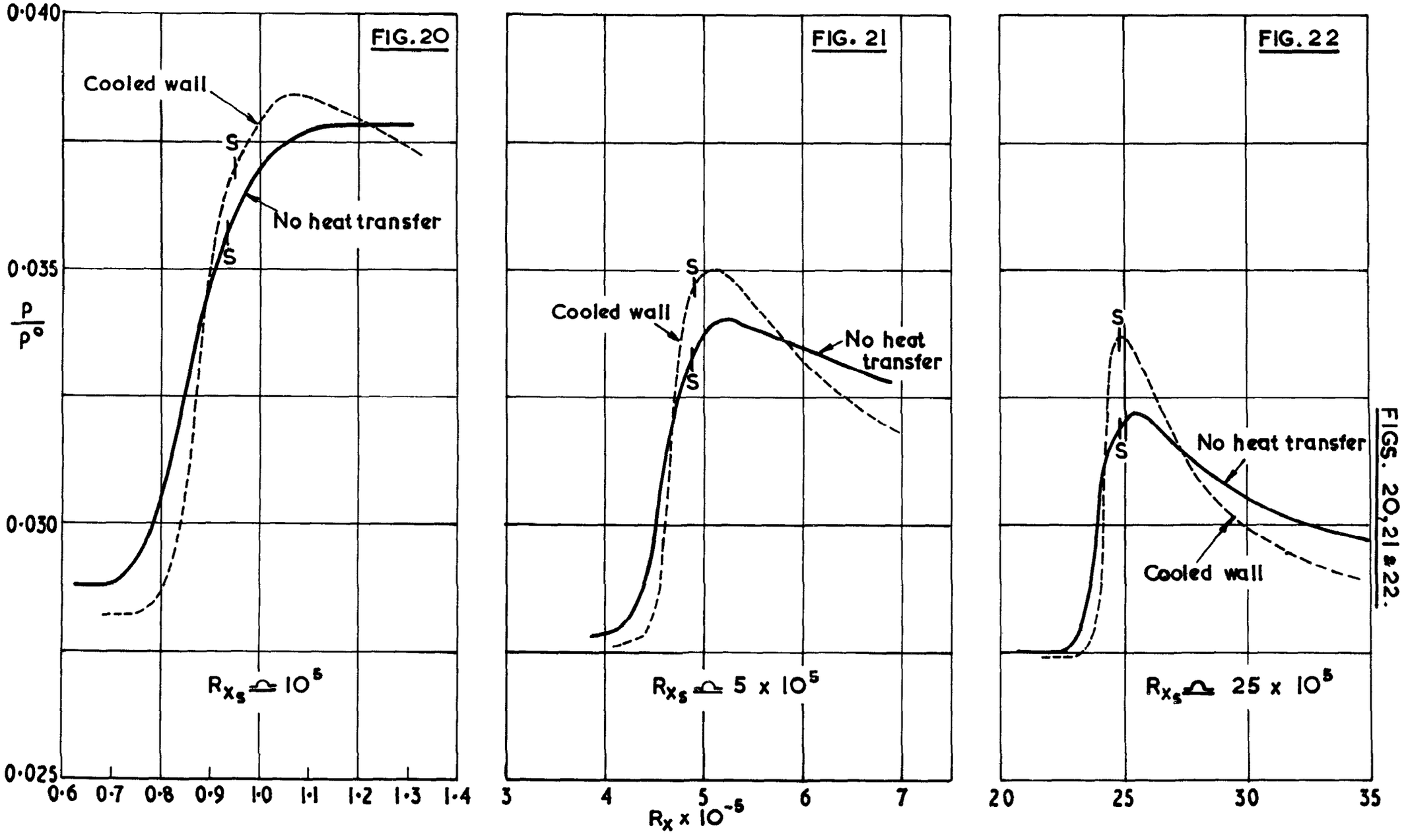

FIGS. 20, 21 & 22.

The laminar foot with and without cooling at $M_o = 3$

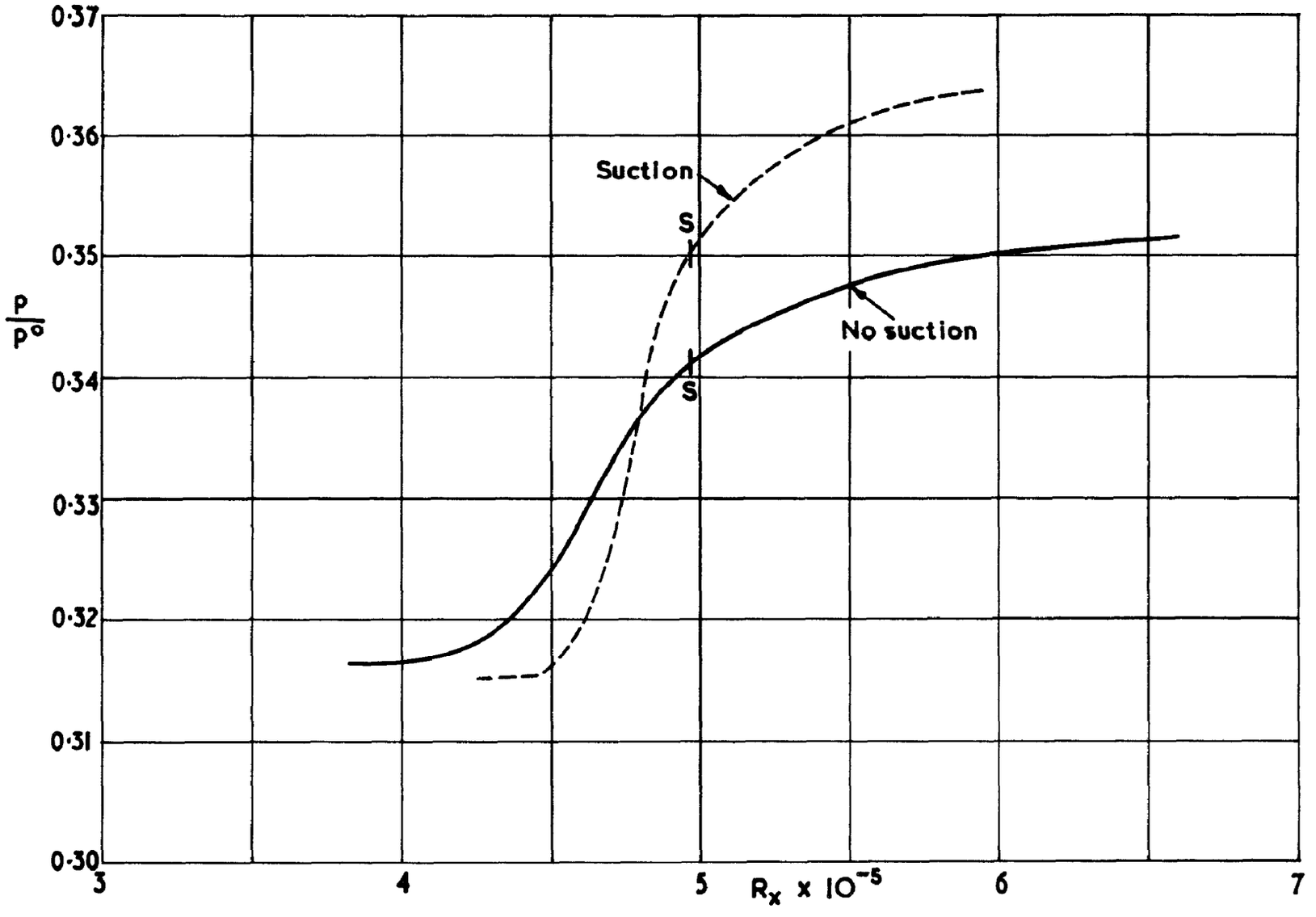

FIG. 23

Calculated effects of suction on a case with incipient separation at $M_o = 1{\cdot}4$

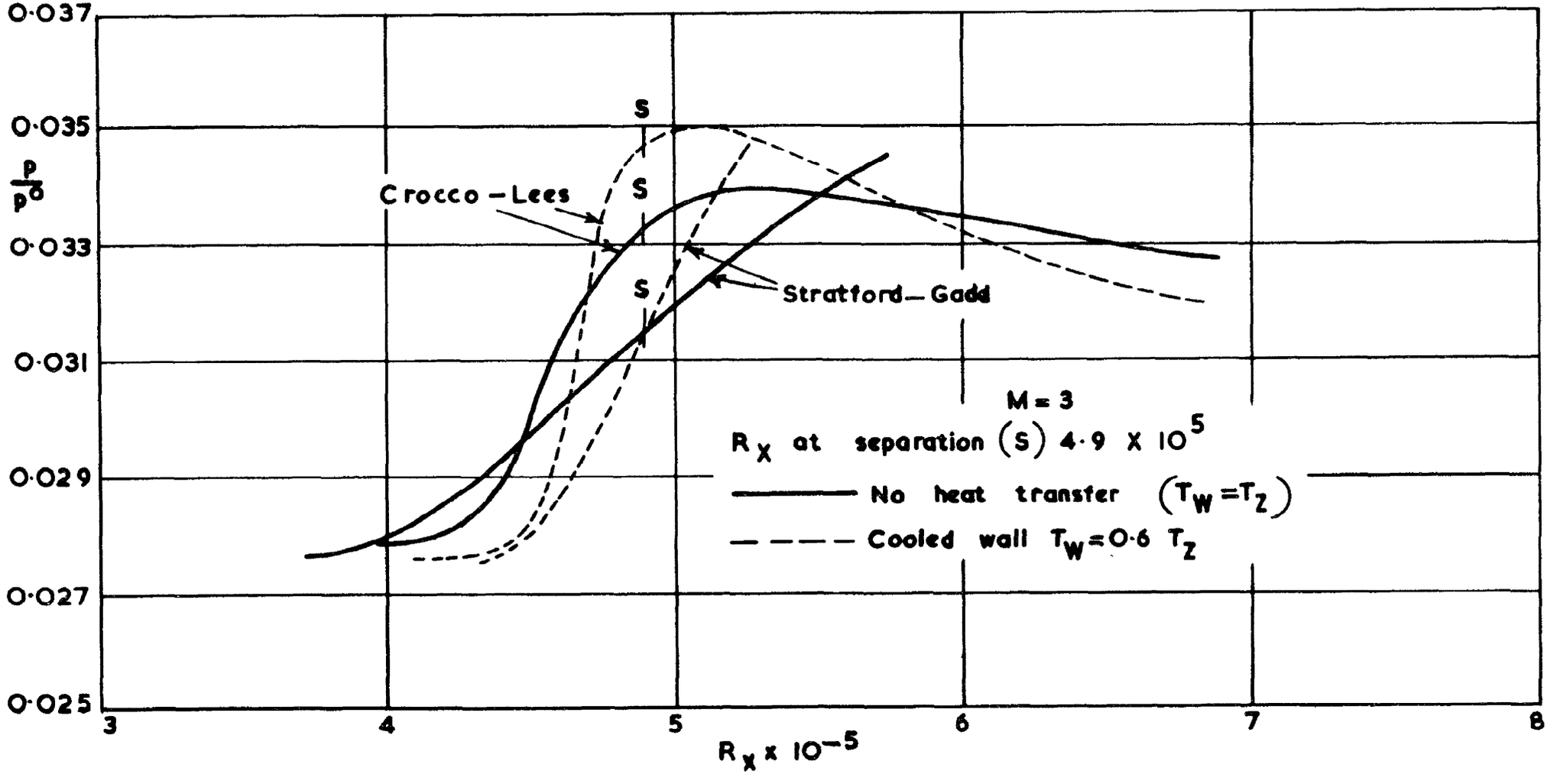

FIG.24.

Theoretical effects of heat transfer on the laminar foot: comparison of theories

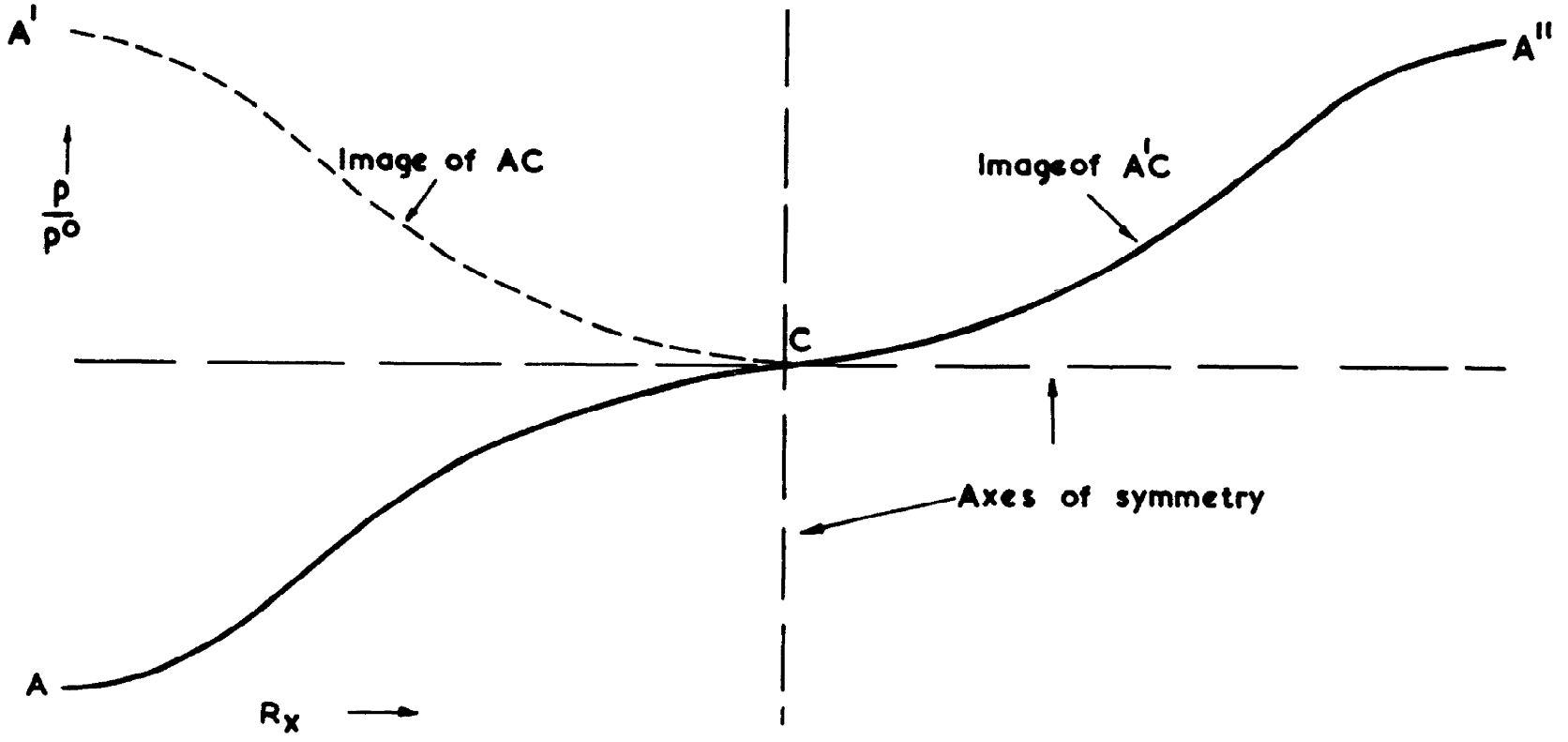

FIG.25.

Pressure distribution doubly reflected in the two axes of symmetry.

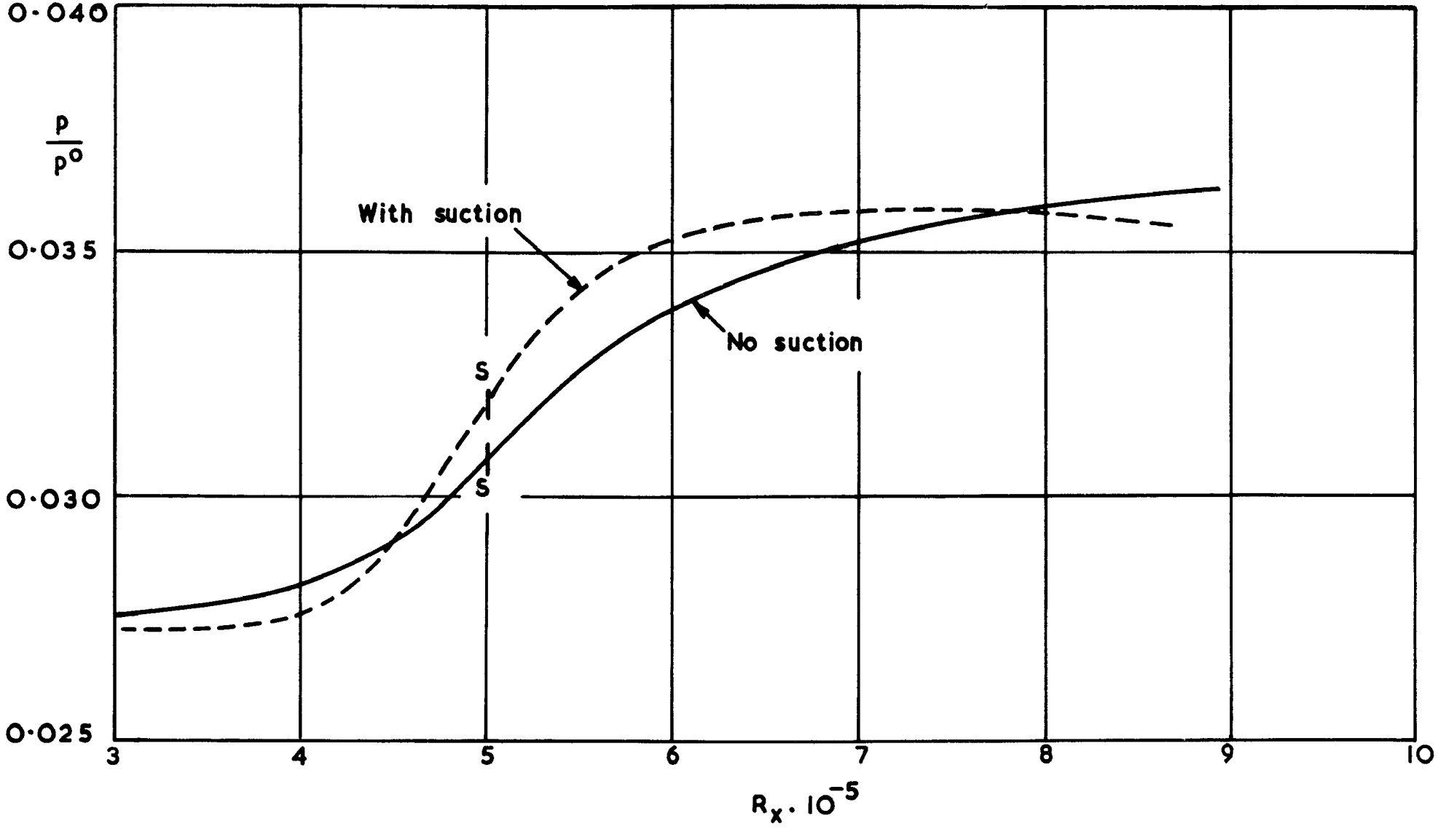

FIG.27

The laminar foot with and without suction at $M_o=3$ and $R_{xs}=5.10^5$, according to the Pohlhausen type of method

A.R.C. C.P. No.556
April, 1960
Bray, K. N. C., Southampton Univ., Gadd, G. E. and Woodger, M., Nat. Phys. Lab.

SOME CALCULATIONS BY THE CROCCO-LEES AND OTHER METHODS OF INTERACTIONS BETWEEN SHOCK WAVES AND LAMINAR BOUNDARY LAYERS, INCLUDING EFFECTS OF HEAT TRANSFER AND SUCTION

The Crocco-Lees method and another method are applied to interactions between shocks and boundary layers that remain laminar throughout. Cooling the wall and the use of distributed suction are both found to reduce the extent of regions of separation.

A.R.C. C.P. No.556
April, 1960
Bray, K. N. C., Southampton Univ., Gadd, G. E. and Woodger, M., Nat. Phys. Lab.

SOME CALCULATIONS BY THE CROCCO-LEES AND OTHER METHODS OF INTERACTIONS BETWEEN SHOCK WAVES AND LAMINAR BOUNDARY LAYERS, INCLUDING EFFECTS OF HEAT TRANSFER AND SUCTION

The Crocco-Lees method and another method are applied to interactions between shocks and boundary layers that remain laminar throughout. Cooling the wall and the use of distributed suction are both found to reduce the extent of regions of separation.

A.R.C. C.P. No.556
April, 1960
Bray, K. N. C., Southampton Univ., Gadd, G. E. and Woodger, M., Nat. Phys. Lab.

SOME CALCULATIONS BY THE CROCCO-LEES AND OTHER METHODS OF INTERACTIONS BETWEEN SHOCK WAVES AND LAMINAR BOUNDARY LAYERS, INCLUDING EFFECTS OF HEAT TRANSFER AND SUCTION

The Crocco-Lees method and another method are applied to interactions between shocks and boundary layers that remain laminar throughout. Cooling the wall and the use of distributed suction are both found to reduce the extent of regions of separation.

A.R.C. C.P. No.556
April, 1960
Bray, K. N. C., Southampton Univ., Gadd, G. E. and Woodger, M., Nat. Phys. Lab.

SOME CALCULATIONS BY THE CROCCO-LEES AND OTHER METHODS OF INTERACTIONS BETWEEN SHOCK WAVES AND LAMINAR BOUNDARY LAYERS, INCLUDING EFFECTS OF HEAT TRANSFER AND SUCTION

The Crocco-Lees method and another method are applied to interactions between shocks and boundary layers that remain laminar throughout. Cooling the wall and the use of distributed suction are both found to reduce the extent of regions of separation.

Printed and published by
HER MAJESTY'S STATIONERY OFFICE

To be purchased from
York House, Kingsway, London w.c.2
423 Oxford Street, London w.1
13A Castle Street, Edinburgh 2
109 St. Mary Street, Cardiff
39 King Street, Manchester 2
50 Fairfax Street, Bristol 1
2 Edmund Street, Birmingham 3
80 Chichester Street, Belfast 1
or through any bookseller

Printed in England

S.O. Code No. 23-9012--56